The reduction of infarct size and the improvement of left ventricular ejection fraction might decrease mechanical stress on the non-infarcted myocardium, which might decrease hypertrophy and dilatation of the non-infarcted myocardium. Since cardiac hypertrophy and dilatation cause diastolic and systolic heart failure, a reduction of infarct size and an increase of left ventricular ejection fraction could mediate beneficial clinical outcomes. However, we need to do another large-scale clinical trial to target clinical outcomes such as cardiovascular death, because our primary aim here was to test the reduction of infarct size. Moreover, Hayashi and colleagues[20] showed that plasma concentrations of angiotensin II, aldosterone, and endothelin-1 were lower in patients given atrial natriuretic peptide than in controls. Sudden exposure to high concentrations of angiotensin II, aldosterone, and endothelin-1 for several days caused vascular or ventricular remodelling, and attenuation of these harmful effects by infusion of atrial natriuretic peptide could reduce the incidence of cardiac death and readmission to hospital for chronic heart failure.[20]

One reason that nicorandil treatment did not limit infarct size in our study could be the size of the dose. Ishii and colleagues[25] have reported that one intravenous administration of a dose of nicorandil that was three times higher than that which we used decreased the infarct size and reduced the rate of cardiovascular death or readmission to hospital for chronic heart failure in 368 patients with acute myocardial infarction.

Patients in the nicorandil study who were given nicorandil orally in the chronic phase had greater increases in left ventricular ejection fraction, irrespective of whether nicorandil was given intravenously or orally. Since microvascular obstruction ten days after myocardial infarction was associated with left ventricular remodelling and poor prognosis, coronary perfusion might be improved by opening KATP channels in coronary blood vessels during the healing stage. The IONA study[35] showed that nicorandil could reduce the incidence of unstable angina in patients with stable angina.

Our finding that treatment with atrial natriuretic peptide in the acute phase reduced the incidence of readmission to hospital for chronic heart failure could help to reduce the physical, medical, and economic burdens on people around the world. Moreover, since intravenous nicorandil in the acute phase, followed by oral administration in the chronic phase, increased the left ventricular ejection fraction, chronic treatment with nicorandil could improve ventricular function for patients with myocardial infarction in the chronic phase.

Several limitations of our study should be discussed. First, physicians knew the random assignment of patients, and treatment for acute myocardial infarction in the chronic phase was not restricted accordingly; this could have affected the difference in nicorandil treatment at the chronic phase. Second, although we planned to do angiography of the left ventricle when patients were admitted to hospital, some hospitals could not take angiographs, because of the additional medical cost. Therefore, baseline angiographs were absent for some patients. Third, the patterns of missing angiography data on left ventriculography differed between the two studies (which were done at different hospitals) and also between the atrial natriuretic peptide group and corresponding placebo group. We cannot explain this difference, but since we did not intervene in this procedure, we believe that it must be due to chance.

Contributors

Department of Cardiology, National Hospital Organisation Ehime National Hospital, Toon, Ehime, Japan (T Otani); Division of Cardiology, National Hospital Organisation Shizuoka Medical Centre, Suntoh-Gun, Shizuoka, Japan (H Yokoyama); Department of Cardiology, Kameda Medical Centre, Kamogawa, Chiba, Japan (Y Hashimoto); Division of Cardiovascular disease of Medicine, Hokkaido Junkanki Hospital, Sapporo, Hokkaido, Japan (N Funayama); Department of Cardiology, Kyushu Kosei Nenkin Hospital, Kitakyushu, Fukuoka, Japan (H Yamamoto); Department of Cardiology, Surugadai Nihon University Hospital, Chiyoda-Ku, Tokyo, Japan (E Tachibana); Department of Cardiology, St Mary's Hospital, Kurume, Fukuoka, Japan (K Yamamoto); Department of Cardiology, Miki City Hospital, Miki, Hyogo, Japan (K Awano); Division of Cardiology, Cardiovascular Centre, Tsuchiya General Hospital, Hiroshima, Hiroshima, Japan (T Sakuma); Department of Cardiology, Himeji Brain and Heart Centre, Himeji, Hyogo, Japan (T Kajiya); Department of Cardiovascular Centre, National Hospital Organisation Kumamoto Medical Centre, Kumamoto, Kumamoto, Japan (K Fujimoto); Department of Cardiology, Fukuyama Cardiovascular Hospital, Fukuyama, Hiroshima, Japan (H Kohno); Division of Cardiology, Tokuyama Central Hospital, Shunan, Yamaguchi, Japan (T Iwami); Division of Cardiology, Mito Saiseikai General Hospital, Mito, Ibaraki, Japan (M Murata); Division of Cardiology, Osaka General Medical Centre, Osaka, Osaka, Japan (M Fukunami); Department of Cardiology, Kobe General Hospital , Kobe , Hyogo, Japan (A Yamamuro); Department of Cardiology, Ogaki Municipal Hospital, Ogaki, Gifu, Japan (T Sone); Heart Centre Division of Cardiology, Social Insurance Kinan Hospital, Tanabe, Wakayama, Japan (Y Okumoto); Department of Circulatory Devision, National Hospital Organisation Ureshino Medical Centre, Ureshino, Saga, Japan (S Hata); Department of Cardiovascular Medicine, Matsuyama Shimin Hospital, Matsuyama, Ehime, Japan (M Abe); Cardiovascular Centre, Anjo Kosei Hospital, Anjo, Aichi, Japan (Y Murata); Cardiovascular Division of Medicine, National Cardiovascular Centre, Suita, Osaka, Japan (S Yasuda); Department of Cardiovascular and Renal Medicine, Saga University Faculty of Medicine, Saga, Saga, Japan (K Node); Department of Cardiology, Kawachi General Hospital, Higashiosaka, Osaka, Japan (M Mishima); Department of Cardiology, Engaru Kousei Hospital, Monbetsu-Gun, Hokkaido, Japan (H Honda); Department of Cardiology, Ehime Prefectural Imabari Hospital, Imabari, Ehime, Japan (H Matsuoka); Department of Cardiology, Tokushima Red Cross Hospital, Komatushima, Tokushima, Japan (Y Hiasa); Department of Cardiology, Musashino Red Cross Hospital, Musashino, Tokyo, Japan (T Miyamoto); Department of Cardiology, Fukuoka University School of Medicine, Fukuoka, Fukuoka, Japan (K Saku); Department of Cardiology, Chiba Emergency Medical Centre, Chiba, Chiba, Japan (I Ishibashi); Department of Cardiology, Saiseikai Fukuoka General Hospital, Fukuoka, Fukuoka, Japan (Y Yamamoto); Department of Cardiology, National Hospital Organisation Ibaraki-Higashi Hospital, Naka-Gun, Ibaraki, Japan (Y Eki); Department of Cardiology, Kawasaki Medical School Hospital, Kurashiki, Okayama, Japan (K Yoshida); Department of Cardiology,

Tokyo Metropolitan Bokutoh General Hospital, Sumida-Ku, Tokyo, Japan (I Kubo); Division of Cardiology, Omura Municipal Hospital, Omura, Nagasaki, Japan (Y Tanioka); Department of Cardiology, National Hospital Organisation Mito Medical Centre, Higashi Ibaraki-gun, Ibaraki, Japan (S Taguchi); Department of Cardiology, Tokyo Medical University, Shinjuku-ku, Tokyo, Japan (A Yamashina); Department of Cardiology, Fukuyama City Hospital, Fukuyama, Hiroshima, Japan (K Hashimoto); Department of Medicine,Nippon Medical School Chiba Hokuso Hospital, Inba-Gun, Chiba, Japan (K Mizuno); Department of Cardiology, Kanazawa Medical University, Kahoku-Gun, Ishikawa, Japan (S Okubo); Department of Internal Medicine,University of Yamanashi Faculty of Medicine, Chuo,Yamanashi, Japan (K Kugiyama); Department of Cardiology, Tsukazaki Memorial Hospital, Himeji, Hyogo, Japan (H Iida); Department of Cardiovascular Science and Medicine, Chiba University Graduate School of Medicine, Chiba, Chiba, Japan (I Komuro); Department of Cardiovascular Medicine, Graduate School of Medical Sciences Kumamoto University, Kumamoto, Kumamoto, Japan (H Ogawa); Department of Cardiology, Shizuoka Prefectural General Hospital, Shizuoka, Shizuoka, Japan (O Doi); Division of Cardiology, Tokyo Metropolitan Geriatric Hospital, Itabashi-Ku, Tokyo, Japan (K Harada); Department of Internal Medicine, Cardiovascular Division, Asahikawa Medical College, Asahikawa, Hokkaido, Japan (N Hasebe); Department of Cardiology, Sasebo City General Hospital, Sasebo, Nagasaki, Japan (T Yamasa); Department of Internal Medicine, Division of Coronary Heart Disease, Hyogo College of Medicine, Nishinomiya, Hyogo, Japan (M Masutani); Department of Cardiovascular Medicine, Graduate School of Medical Sciences Kyushu University, Fukuoka, Fukuoka, Japan (K Egashira); Department of Cardiovascular Medicine, Tokyo Medical and Dental University, Bunkyo-Ku, Tokyo, Japan (M Isobe); Department of Internal Medicine and Cardiology, Graduate School of Medicine Osaka City University, Osaka, Osaka, Japan (M Yoshiyama); Department of Cardiology, Tokyo Women's Medical University, Shinjyuku-Ku, Tokyo, Japan (H Kasanuki); Department of Cardiology, Nagasaki Citizens Hospital, Nagasaki, Nagasaki, Japan (S Suzuki); Department of Emergency and Critical Care Medicine, Chikushi Hospital Fukuoka University, Chikushino, Fukuoka, Japan (H Mihara).

Conflict of interest statement

We declare that we have no conflict of interest.

Acknowledgments

These studies were supported by grants for Comprehensive Research on Ageing and Health (H13-21seiki (seikatsu) 23), in Health and Labour Sciences Research from Ministry of Health, Labour and Welfare, Japan, and by a grant from the Japanese Cardiovascular Research Foundation. We thank Satomi Ihara for her excellent assistance with data management; Hidetoshi Okazaki, Hiroyuki Yamamoto, Masakatsu Wakeno, Atsushi Nakano, Hiroyuki Takahama, Shin Ito, Hideyuki Sasaki, and Kyungduk Min for analysis of angiographs of left ventricles; Yoshie Yanagi, Hiromi Ohara, Chikayo Tsujimoto, Naoko Matsuo, Yoshihiro Asano, Masashi Fujita, Shuichiro Higo, and Mitsutoshi Asai for data monitoring; Ms Uchida at SACT international for data analysis; Dr Tsutomu Yamazaki for data management; and Dr Ed Schweitzer for review of the manuscript.

References

1 Thom T, Haase N, Rosamond W, et al. Heart disease and stroke statistics–2006 update: a report from the American Heart Association Statistics Committee and Stroke Statistics Subcommittee. *Circulation* 2006; **113**: 85–151.

2 Jessup M, Brozena S. Heart failure. *N Engl J Med* 2003; **348**: 2007–18.

3 Levy D, Kenchaiah S, Larson MG, et al. Long-term trends in the incidence of and survival with heart failure. *N Engl J Med* 2002; **347**: 1397–402.

4 Shiba N, Watanabe J, Shinozaki T, et al. Poor prognosis of Japanese patients with chronic heart failure following myocardial infarction—comparison with nonischemic cardiomyopathy. *Circ J* 2005; **69**: 143–49.

5 Kloner RA, Rezkalla SH. Cardiac protection during acute myocardial infarction: where do we stand in 2004? *J Am Coll Cardiol* 2004; **44**: 276–86.

6 The MIAMI Trial Research Group. Metoprolol in acute myocardial infarction (MIAMI). A randomised placebo-controlled international trial. *Eur Heart J* 1985; **6**: 199–226.

7 Ross AM, Gibbons RJ, Stone GW, Kloner RA, Alexander RW. A randomised, double-blinded, placebo-controlled multicenter trial of adenosine as an adjunct to reperfusion in the treatment of acute myocardial infarction (AMISTAD-II). *J Am Coll Cardiol* 2005; **45**: 1775–80.

8 van der Horst IC, Zijlstra F, van't Hof AW, et al. Glucose-insulin-potassium infusion inpatients treated with primary angioplasty for acute myocardial infarction: the glucose-insulin-potassium study: a randomised trial. *J Am Coll Cardiol* 2003; **42**: 784–91.

9 Grines CL, Browne KF, Marco J, et al. A comparison of immediate angioplasty with thrombolytic therapy for acute myocardial infarction. The Primary Angioplasty in Myocardial Infarction Study Group. *N Engl J Med* 1993; **328**: 673–79.

10 Sakurai K, Watanabe J, Iwabuchi K, et al. Comparison of the efficacy of reperfusion therapies for early mortality from acute myocardial infarction in Japan: registry of Miyagi Study Group for AMI (MsAMI). *Circ J* 2003; **67**: 209–14.

11 Lamas GA, Flaker GC, Mitchell G, et al. Effect of infarct artery patency on prognosis after acute myocardial infarction. The Survival and Ventricular Enlargement Investigators. *Circulation* 1995; **92**: 1101–09.

12 Verma S, Fedak PW, Weisel RD, et al. Fundamentals of reperfusion injury for the clinical cardiologist. *Circulation* 2002; **105**: 2332–36.

13 Zeymer U, Suryapranata H, Monassier JP, et al. The Na(+)/H(+) exchange inhibitor eniporide as an adjunct to early reperfusion therapy for acute myocardial infarction. Results of the evaluation of the safety and cardioprotective effects of eniporide in acute myocardial infarction (ESCAMI) trial. *J Am Coll Cardiol* 2001; **38**: 1644–50.

14 European Study of Prevention of Infarct with Molsidomine (ESPRIM) Group. The ESPRIM trial: short-term treatment of acute myocardial infarction with molsidomine. *Lancet* 1994; **344**: 91–97.

15 Wall TC, Califf RM, Blankenship J, et al. Intravenous fluosol in the treatment of acute myocardial infarction. Results of the Thrombolysis and Angioplasty in Myocardial Infarction 9 Trial. TAMI 9 Research Group. *Circulation* 1994; **90**: 114–20.

16 Cody RJ, Atlas SA, Laragh JH, et al. Atrial natriuretic factor in normal subjects and heart failure patients. Plasma levels and renal, hormonal, and hemodynamic responses to peptide infusion. *J Clin Invest* 1986; **78**: 1362–74.

17 Emori T, Hirata Y, Imai T, Eguchi S, Kanno K, Marumo F. Cellular mechanism of natriuretic peptides-induced inhibition of endothelin-1 biosynthesis in rat endothelial cells. *Endocrinology* 1993; **133**: 2474–80.

18 Kitakaze M, Minamino T, Node K, et al. Role of activation of ectosolic 5′-nucleotidase in the cardioprotection mediated by opening of K+ channels. *Am J Physiol* 1996; **270**: 1744–56.

19 Mizumura T, Nithipatikorn K, Gross GJ. Infarct size-reducing effect of nicorandil is mediated by the KATP channel but not by its nitrate-like properties in dogs. *Cardiovasc Res* 1996; **32**: 274–85.

20 Hayashi M, Tsutamoto T, Wada A, et al. Intravenous atrial natriuretic peptide prevents left ventricular remodeling in patients with first anterior acute myocardial infarction. *J Am Coll Cardiol* 2001; **37**: 1820–26.

21 Kuga H, Ogawa K, Oida A, et al. Administration of atrial natriuretic peptide attenuates reperfusion phenomena and preserves left ventricular regional wall motion after direct coronary angioplasty for acute myocardial infarction. *Circ J* 2003; **67**: 443–48.

22 Sugimoto K, Ito H, Iwakura K, et al. Intravenous nicorandil in conjunction with coronary reperfusion therapy is associated with better clinical and functional outcomes in patients with acute myocardial infarction. *Circ J* 2003; **67**: 295–300.

23 Sakata Y, Kodama K, Komamura K, et al. Salutary effect of adjunctive intracoronary nicorandil administration on restoration of myocardial blood flow and functional improvement in patients with acute myocardial infarction. *Am Heart J* 1997; **133**: 616–21.

24 Fukuzawa S, Ozawa S, Inagaki M, et al. Nicorandil affords cardioprotection in patients with acute myocardial infarction treated with primary percutaneous transluminal coronary angioplasty: assessment with thallium-201/iodine-123 BMIPP dual SPECT. *J Nucl Cardiol* 2000; **7**: 447–53.

25 Ishii H, Ichimiya S, Kanashiro M, et al. Impact of a single intravenous administration of nicorandil before reperfusion in patients with ST-segment-elevation myocardial infarction. *Circulation* 2005; **112**: 1284–88.

26 Asakura M, Jiyoong K, Minamino T, Shintani Y, Asanuma H, Kitakaze M. Rationale and design of a large-scale trial using atrial natriuretic peptide (ANP) as an adjunct to percutaneous coronary intervention for ST-segment elevation acute myocardial infarction: Japan-Working groups of acute myocardial infarction for the reduction of Necrotic Damage by ANP (J-WIND-ANP). *Circ J* 2004; **68**: 95–100.

27 Minamino T, Jiyoong K, Asakura M, Shintani Y, Asanuma H, Kitakaze M. Rationale and design of a large-scale trial using nicorandil as an adjunct to percutaneous coronary intervention for ST-segment elevation acute myocardial infarction: Japan-Working groups of acute myocardial infarction for the reduction of Necrotic Damage by a K-ATP channel opener (J-WIND-KATP). *Circ J* 2004; **68**: 101–06.

28 Seino Y, Tomita Y, Hoshino K, Setsuta K, Takano T, Hayakawa H. Pathophysiological analysis of serum troponin T release kinetics in evolving ischemic myocardial injury. *Jpn Circ J* 1996; **60**: 265–76.

29 Steen H, Giannitsis E, Futterer S, Merten C, Juenger C, Katus HA. Cardiac troponin T at 96 hours after acute myocardial infarction correlates with infarct size and cardiac function. *J Am Coll Cardiol* 2006; **48**: 2192–94.

30 Vollmer RT, Christenson RH, Reimer K, Ohman EM. Temporal creatine kinase curves in acute myocardial infarction. Implications of a good empiric fit with the log-normal function. *Am J Clin Pathol* 1993; **100**: 293–98.

31 Therneau TM, Grambsch PM. Modeling survival data: extending the Cox model. New York, USA: Springer, 2000.

32 Hess KR. Graphical methods for assessing violations of the proportional hazards assumption in Cox regression. *Stat Med* 1995; **14**: 1707–23.

33 Mahaffey KW, Puma JA, Barbagelata NA, et al. Adenosine as an adjunct to thrombolytic therapy for acute myocardial infarction: results of a multicenter, randomised, placebo-controlled trial: the Acute Myocardial Infarction STudy of ADenosine (AMISTAD) trial. *J Am Coll Cardiol* 1999; **34**: 1711–20.

34 Grover GJ, Sleph PG, Dzwonczyk S. Role of myocardial ATP-sensitive potassium channels in mediating preconditioning in the dog heart and their possible interaction with adenosine A1-receptors. *Circulation* 1992; **86**: 1310–16.

35 IONA Study Group. Effect of nicorandil on coronary events in patients with stable angina: the Impact Of Nicorandil in Angina (IONA) randomised trial. *Lancet* 2002; **359**: 1269–75.

Increased Endoplasmic Reticulum Stress in Atherosclerotic Plaques Associated With Acute Coronary Syndrome

Masafumi Myoishi, MD; Hiroyuki Hao, MD, PhD; Tetsuo Minamino, MD, PhD; Kouki Watanabe, MD, PhD; Kensaku Nishihira, MD, PhD; Kinta Hatakeyama, MD, PhD; Yujiro Asada, MD, PhD; Ken-ichiro Okada, MD, PhD; Hatsue Ishibashi-Ueda, MD, PhD; Giulio Gabbiani, MD, PhD; Marie-Luce Bochaton-Piallat, PhD; Naoki Mochizuki, MD, PhD; Masafumi Kitakaze, MD, PhD

Background—The endoplasmic reticulum (ER) responds to various stresses by upregulation of ER chaperones, but prolonged ER stress eventually causes apoptosis. Although apoptosis is considered to be essential for the progression and rupture of atherosclerotic plaques, the influence of ER stress and apoptosis on rupture of unstable coronary plaques remains unclear.

Methods and Results—Coronary artery segments were obtained at autopsy from 71 patients, and atherectomy specimens were obtained from 40 patients. Smooth muscle cells and macrophages in the fibrous caps of thin-cap atheroma and ruptured plaques, but not in the fibrous caps of thick-cap atheroma and fibrous plaques, showed a marked increase of ER chaperone expression and apoptotic cells. ER chaperones also showed higher expression in atherectomy specimens from patients with unstable angina pectoris than in specimens from those with stable angina. Expression of 7-ketocholesterol was increased in the fibrous caps of thin-cap atheroma compared with thick-cap atheroma. Treatment of cultured coronary artery smooth muscle cells or THP-1 cells with 7-ketocholesterol induced upregulation of ER chaperones and apoptosis, whereas these changes were prevented by antioxidants. We also investigated possible signaling pathways for ER-initiated apoptosis and found that the CHOP (a transcription factor induced by ER stress)-dependent pathway was activated in unstable plaques. In addition, knockdown of CHOP expression by small interfering RNA decreased ER stress-dependent death of cultured coronary artery smooth muscle cells and THP-1 cells.

Conclusions—Increased ER stress occurs in unstable plaques. Our findings suggest that ER stress-induced apoptosis of smooth muscle cells and macrophages may contribute to plaque vulnerability. (***Circulation*. 2007;116:1226-1233.**)

Key Words: apoptosis ■ plaque ■ myocardial infarction ■ endoplasmic reticulum

Most of the acute clinical manifestations of coronary atherosclerosis result from plaque rupture that triggers thrombosis and vessel occlusion, producing the acute coronary syndrome (ACS).[1–3] Previous reports have shown that apoptosis affects all of the types of cells residing within atherosclerotic plaques, including smooth muscle cells (SMCs) and macrophages,[4,5] with oxidized low-density lipoprotein and several inflammatory factors being known to induce apoptosis.[6,7] The number of apoptotic cells depends on the plaque stage and is generally higher in more advanced plaques.[6,8] SMCs synthesize most of the interstitial collagen that stabilizes the fibrous cap of a plaque.[4,7] Therefore, excessive apoptosis of SMCs in the fibrous cap may compromise plaque integrity and render it vulnerable to proteolytic attack by inflammatory cells, leading to plaque rupture.[4,7] Apoptotic macrophages are more frequent at sites of plaque rupture than in areas where the fibrous cap remains intact.[9] A decrease in macrophages would reduce the scavenging of apoptotic SMCs and macrophages, allowing the cells to undergo secondary necrosis, thereby increasing thrombogenicity of the plaque.[10]

Editorial p 1214
Clinical Perspective p 1233

The endoplasmic reticulum (ER) is 1 of the largest cellular organelles and has multiple functions, such as regulating the folding of proteins.[11,12] Various stimuli cause ER stress,

Received December 10, 2006; accepted July 6, 2007.

From the Departments of Cardiovascular Medicine (M.M., M.K.), Structural Analysis (M.M., N.M.), and Pathology (H.H., H.I.-U.), National Cardiovascular Center, Suita, Osaka, Japan; Department of Surgical Pathology (H.H.), Hyogo College of Medicine, Nishinomiya, Hyogo, Japan; Departments of Bioregulatory Medicine (M.M.) and Cardiovascular Medicine (T.M., K.-i.O.), Osaka University Graduate School of Medicine, Suita, Osaka, Japan; Division of Cardiology (K.W.), Uwajima City Hospital, Uwajima, Ehime, Japan; Department of Pathology (K.N., K.H., Y.A.), Faculty of Medicine, University of Miyazaki, Miyazaki, Japan; and Department of Pathology and Immunology (G.G., M.-L.B.-P.), University of Geneva–CMU, Geneva, Switzerland.

The online-only Data Supplement, consisting of expanded Methods, tables, and figures, is available with this article at http://circ.ahajournals.org/cgi/content/full/CIRCULATIONAHA.106.682054/DC1.

Correspondence to Masafumi Kitakaze, MD, PhD, Department of Cardiovascular Medicine, National Cardiovascular Center, Suita, Osaka 565-8565, Japan. E-mail kitakaze@zf6.so-net.ne.jp

Circulation **is available at http://circ.ahajournals.org**

DOI: 10.1161/CIRCULATIONAHA.106.682054

including ischemia, hypoxia, heat shock, mutation, increased protein synthesis, and reactive oxygen species, all of which can potentially lead to ER dysfunction.[11,12] In response to ER stress, there is marked upregulation of various ER chaperones, such as the 94-kDa glucose-regulated protein (GRP94) or GRP78 that stabilizes protein folding.[11,13,14] When the ER becomes overloaded with misfolded proteins, the unfolded protein response (UPR) occurs to enhance cell survival.[15] However, prolonged ER stress can trigger apoptotic cell death, which is promoted by transcriptional induction of C/EBP homologous protein (CHOP) and/or by the activation of c-JUN NH_2-terminal kinase (JNK)– and/or caspase-12–dependent pathways.[16] In support of this concept, our investigation of the effects of prolonged ER stress on hypertrophic and failing hearts revealed that apoptosis of cardiac myocytes was induced via activation of CHOP, an ER-specific proapoptotic factor.[17] An important role of ER-initiated cell death pathways has also been demonstrated in several diseases, including diabetes mellitus,[16] neurodegenerative conditions,[18] and ischemia.[19]

Oxidation of low-density lipoprotein plays a significant pathogenetic role in atherosclerosis.[6,7,20] In cultured peritoneal macrophages, excessive accumulation of free cholesterol (induced by acetyl low-density lipoprotein with an acyl-CoA:cholesterol acyltransferase [ACAT] inhibitor) initiates ER stress, increases CHOP expression, and leads to apoptosis.[21] Studies of $apoE^{-/-}$ mice also support the relevance of ER stress to macrophage apoptosis and to enlargement of the necrotic core in advanced atherosclerotic plaques.[22,23] However, it is still unclear whether ER stress and UPR activation have a role in plaque rupture. Unfortunately, the absence of a suitable animal model has greatly hindered investigation of the molecular mechanisms of plaque rupture and evaluation of the effects of ER stress in vivo.[24,25]

In the present study, we examined histological sections from atherosclerotic coronary artery lesions obtained at autopsy or after directional coronary atherectomy (DCA) to investigate markers of ER stress/UPR activation and apoptotic cell death. Oxysterols such as 7-ketocholesterol (7-KC) have been reported to be partially responsible for the cytotoxicity of oxidized low-density lipoprotein.[26,27] Exposure of cultured human SMCs to 7-KC induces the UPR and promotes apoptotic cell death,[28] so we investigated 7-KC expression in plaque specimens by immunohistochemistry. We also examined whether 7-KC could activate ER stress using cultured human coronary artery SMCs (CASMCs) and a monocyte cell line (THP-1). Furthermore, we investigated the possible signaling pathways for ER-initiated apoptosis, and we found that the CHOP (a transcription factor induced by ER stress)-dependent pathway was activated in unstable plaques, whereas knockdown of CHOP expression by small interfering RNA (siRNA) decreased ER stress-dependent death of cultured CASMCs and THP-1 cells.

Methods

Coronary Artery Specimens

Two different sets of specimens were obtained under a protocol approved by the Institutional Review Board of the National Cardiovascular Center and Miyazaki University. The first set of specimens was obtained at autopsy, and the second set was obtained by DCA. Classification of the histology of the lesions in autopsy specimens was done morphologically, as described previously (Table 1).[29–31] Demographic data for the study population are presented in Table I of the Data Supplement.

TABLE 1. Human Coronary Specimens (Autopsy; n=71)

Histological Classification of Lesions	No. of Specimens	AHA Classification
No. of specimens obtained at autopsy	152	...
Diffuse intimal thickening (normal)	21	Type I
Fibrous plaques (fibrous)	48	Type Vc
Thick-cap atheroma (thick)	51	Type Va
Thin-cap atheroma (thin)	15	Type Va
Ruptured plaques (ruptured)	17	Type VI

AHA Classification indicates American Heart Association histological criteria.[30,31]

In brief, 152 coronary artery segments were obtained at autopsy from 71 patients, including 17 consecutive patients who experienced fatal ACS without percutaneous coronary intervention and 54 consecutive patients with noncardiac death. The major coronary arteries and their branches were cut transversely at ≈5-mm intervals, and 17 ruptured plaques were detected in the 17 ACS patients (ruptured: AHA type VI, n=17). The remaining 33 patients with noncardiac death and the 17 ACS patients also had advanced unruptured plaques (≥75% cross-sectional luminal narrowing), and we assessed each segment at the narrowest point (n=114). The advanced atherosclerotic unruptured plaques were additionally divided into fibrous plaques (fibrous: fibrocellular tissue was the predominant component, and the lipid core was inconspicuous or absent; AHA type Vc, n=48), thick-cap atheroma (thick: a lipid core covered by a fibrous cap >65-μm thick; AHA type Va, n=51), and thin-cap atheroma (thin: a lipid-rich core covered by a fibrous cap <65-μm thick[32]; AHA type Va, n=15). Another 21 patients with noncardiac death who had no advanced unruptured plaques and normal coronary arteries that only showed diffuse intimal thickening (normal: AHA type I, n=21) were used as a control group.

We performed a morphological analysis of multiple lesions (n=152) obtained at autopsy from 71 patients (Figure 1). The supplementary analyses included pairwise comparison of unruptured and ruptured plaques from each heart of each patient with ACS (Data Supplement Figure I) and investigation of the correlation between traditional cardiovascular risk factors and ER stress (Data Supplement Table II and Figure III). These supplementary analyses were based on representative data from each patient. (Details of the methods used to perform the supplementary analyses are included in the expanded Methods section in the Data Supplement.)

Forty DCA specimens were obtained from 40 patients who were treated for stable angina pectoris (SAP; n=20) or unstable angina pectoris (UAP; n=20). One DCA specimen was obtained per patient, and these specimens were classified on the basis of the clinical situation at the time of DCA (Table 2). These specimens were fixed in 4% paraformaldehyde for 6 hours at 4°C and then embedded in paraffin.

Immunohistochemistry

Serial sections were examined by immunohistochemistry, as described previously.[17] In brief, sections were deparaffinized, and endogenous peroxidase activity was blocked by incubation with 0.3% H_2O_2 in methanol for 30 minutes. For some antibodies, antigen retrieval was performed as specified below. After blocking with 3% normal bovine serum albumin, sections were incubated with the primary antibody overnight at 4°C. KDEL (Lys-Asp-Glu-Leu) antibody, which recognizes both GRP78 and GRP94, was purchased from Stressgen (San Diego, Calif) and was used at a dilution of 1:2000. Anti-CHOP antibody was obtained from Santa Cruz Biotechnology (Santa Cruz, Calif) and was applied at a dilution of 1:600

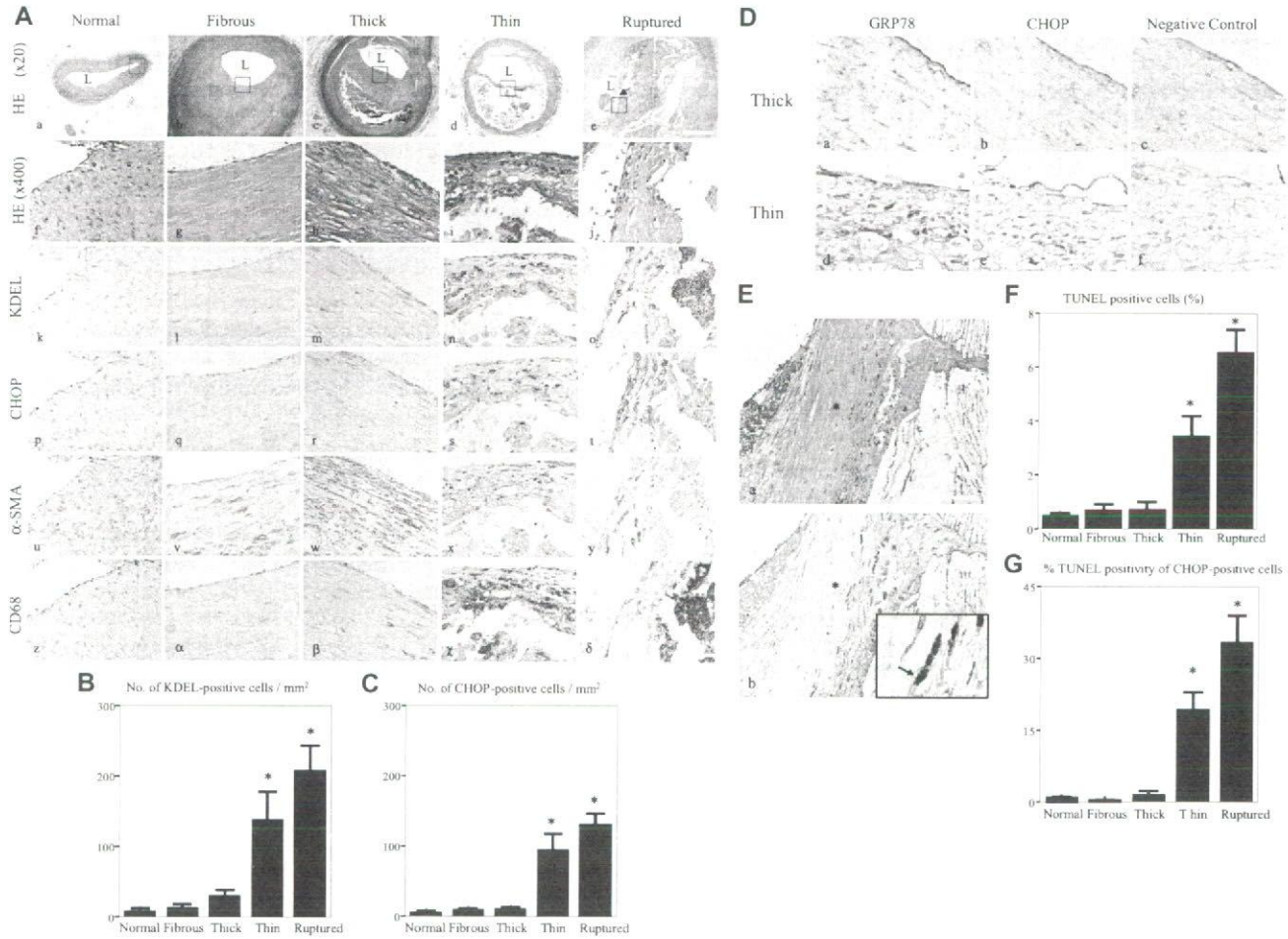

Figure 1. Induction of ER chaperones and death signals in coronary artery plaques obtained at autopsy. A, Comparison of hematoxylin-eosin (HE) staining, KDEL immunostaining, and CHOP immunostaining of normal arteries (n=14), fibrous plaques (n=48), thick-cap atheroma (n=51), thin-cap atheroma (n=15), and ruptured plaques (n=17) obtained at autopsy from 71 patients. Representative HE-stained low-power micrographs from each group (a through e). L indicates the lumen, and the arrow shows the site of plaque rupture. The parts of the intima (a) and fibrous cap (b through e) indicated by boxes are shown at a higher magnification in panels f through j. Panels k through o show KDEL immunostaining. Panels p through t show CHOP immunostaining. Panels u through y show α-smooth muscle actin (α-SMA) immunostaining. Panels z through δ show CD68 immunostaining. B and C, The number of KDEL-positive (B) and CHOP-positive (C) cells. The absolute number per square millimeter is shown for the media of a normal artery and for the fibrous caps of fibrous plaques, thick-cap atheroma, thin-cap atheroma, and ruptured plaques (B, C). D, ISH analysis of GRP78 (a, d), CHOP (b, e), and negative control (c, f) mRNA expression in thick- and thin-cap atheromas. E, Comparison of HE staining (a) with double immunostaining (b). Colocalization of CHOP (red) with TUNEL-positive cells (brown) in the cap of a ruptured plaque. The area indicated by asterisks is shown at a higher magnification in the inset. Arrows show CHOP and TUNEL double-positive cells. F and G, Percentage of TUNEL-positive cells (F) and percentage of TUNEL-positive cells among CHOP-positive cells (G) in the fibrous cap. Scale bars represent 1 mm (A, a through e), 50 μm (A, f through δ, D, and E), and 20 μm (E, in inset). *$P<0.05$ vs normal plaque.

after antigen retrieval by incubation for 10 minutes at room temperature in 5 μg/mL proteinase K. Anti-phospho-c-JUN NH_2-terminal kinase antibody was used to detect c-JUN kinase (JNK), which is involved in the UPR.[16] It was obtained from Cell Signaling (Danvers, Mass) and was applied at a dilution of 1:100 after heat retrieval for 15 minutes at a sub-boiling temperature in 1 mmol/L EDTA (pH 8.0). Colon carcinoma sections were stained with anti-phospho-JNK antibody as a positive control. Anti-α-smooth muscle actin antibody and anti-human CD68 antibody (DAKO, Glostrup, Denmark) were used to identify SMCs and macrophages, respectively, and were used at a dilution of 1:200. The EnVision kit (DAKO) was then used for immunostaining. Application of the KDEL antibody or the CHOP antibody after preincubation with each synthetic peptide used for immunization (KDEL: synthetic peptide SEKDEL, 10 μg/mL, Tore Bio, CHOP peptide: 10 μg/mL, Santa Cruz Biotechnology) resulted in no detectable signals, demonstrating the specificity of the antibody (Data Supplement Figure II).

TABLE 2. Human Coronary Specimens (Atherectomy; n=40)

Origin and Classification of Plaques	No. of Specimens
SAP	20
UAP	20

Terminal dUTP Nick End-Labeling Method and Double Immunohistochemistry

Cells undergoing apoptosis were identified by the terminal dUTP nick end-labeling (TUNEL) method with the ApopTag In Situ Apoptosis Detection Kit (Chemicon, Temecula, Calif), as described previously.[8] For simultaneous identification of CHOP and TUNEL immunoreactivity, double immunostaining of specimens was performed. First, the TUNEL method was performed with an ApopTag

kit, and then CHOP was detected with an alkaline phosphatase–labeled secondary antibody with NewFukusin (DAKO).

In Situ Hybridization

Digoxigenin-labeled cRNA probes and the negative control (LNE120) were purchased from Direct Communications Inc (Hirosaki, Japan), and the sequences were as follows: GRP78: 5′-UGGAAUUCGAGUCGAGCCACCAACAAGAACAAUUUCAUCAAUAUCAGACUUCUUCAAAUCAGAAUCUUCCAACACUUUCUGGACGGGCUUCAUAGUAGACCGGAACAGAUCCA UGUUGAG-3′; CHOP: 5′-AUGCUCCCAAUUGUUCAUGCUUGGUGCAGAUUCACCAUUCGGUCAAUCAGAGCUCGGCGAGUCGCCUCUACUUCCCUGGUCAGGCGCUCGAUUUCCUGCUUGAGCCGUUCAUUCUCUUC-3′. In situ hybridization (ISH) was performed as described previously[33] with a Microprobe manual staining system (Fisher Scientific, Pittsburgh, Pa). In brief, hybridization of the probes (1 μg/mL) was performed for 120 minutes at 50°C, and then anti-digoxigenin-Ap (x250, Roche, Basel, Switzerland), as the secondary antibody, and NBT/BCIP stock solution (×50, Roche) were added.

7-KC Staining

Snap-frozen samples were obtained from 12 patients, comprising 6 with thick-cap atheroma and 6 with thin-cap atheroma. Frozen sections were fixed in 10% neutral-buffered formalin for 1 hour at room temperature. After blocking with 3% normal bovine serum albumin, the sections were incubated overnight at 4°C with anti-7-KC antibody (Nikken Seil Corporation, Fukuroi, Japan) at a dilution of 1:100, followed by incubation with an EnVision kit for 30 minutes.

Statistical Analysis

Data are expressed as mean±SEM. For the autopsy study of multiple lesions from many patients (Figure 1), statistical analysis was performed with the Kruskal–Wallis *H* test and a post hoc Mann-Whitney *U* test. For the DCA specimens, statistical analysis was performed with the Mann-Whitney *U* test. Experiments with cultured cells were performed at least 3 times each. Data obtained with cultured cells were analyzed statistically by the unpaired Student *t* test or ANOVA, followed by the Bonferroni test. Comparison of categorical variables was done with Fisher exact test. In all analyses, $P<0.05$ was accepted as statistically significant. The expanded Methods section, covering supplementary data and in vitro studies is included as an online-only Data Supplement.

The authors had full access to and take full responsibility for the integrity of the data. All authors have read and agree to the manuscript as written.

Results

Upregulation of ER Chaperones and Apoptosis in the Fibrous Caps of Thin-Cap Atheroma and Ruptured Plaques

In the fibrous caps of thin-cap atheroma and ruptured plaques, KDEL and CHOP immunostaining showed a marked increase compared with the level of staining in the fibrous caps of thick-cap atheroma and fibrous plaques (Figure 1A k through t, Figure 1B, and Figure 1C). KDEL-positive cells were more numerous than CHOP-positive cells in the fibrous caps of thin-cap atheroma and ruptured plaques. Most of the CHOP-positive cells also expressed KDEL, as shown by staining of serial sections. In the same hearts of the ACS patients, there was a significant difference of KDEL- and CHOP-positive cells between the unruptured and ruptured plaques (Data Supplement Figure I). We also assessed ER chaperone (GRP78) and CHOP expression at the mRNA level by ISH (Figure 1D). Furthermore, we confirmed that the KDEL- and CHOP-positive cells were SMCs or macrophages by immunostaining of serial sections with anti α-smooth muscle actin and anti-CD68, respectively (Figure 1A, u through δ). In the fibrous caps of thin-cap atheroma and ruptured plaques, colocalization of CHOP immunoreactivity with TUNEL-positive cells was observed by double immunostaining (Figure 1E). The percentage of TUNEL-positive cells (Figure 1F) and the percentage of TUNEL-positive cells among CHOP-positive cells (Figure 1G) were increased compared with the findings in other specimens. Immunostaining for phospho-JNK, which is a proapoptotic factor involved in ER stress, revealed no immunoreactivity in the fibrous caps of thick, thin, or ruptured plaques (data not shown). In normal coronary artery specimens with diffuse intimal thickening (Figure 1A, k and p), there was no KDEL or CHOP positivity. In the region around the necrotic core of advanced plaques, KDEL positivity was only observed in macrophages. There was no significant difference in the number of KDEL-positive cells within the area surrounding the necrotic core of thick-cap atheromas (726±88/mm^2), thin-cap atheromas (741±52/mm^2), and ruptured plaques (651±102/mm^2).

Upregulation of ER Stress in Atherectomy Specimens From Patients With UAP

To estimate the activation of ER stress related to the clinical situation, we examined histological sections obtained at DCA. Morphometric analysis demonstrated that the number of KDEL- and CHOP-positive cells was significantly higher in patients with UAP than in patients with SAP ($P<0.05$; Figures 2A, 2B, and 2C). The KDEL- and CHOP-positive cells were confirmed to be SMCs and macrophages (Figure 2A). When ER chaperone (GRP78) and CHOP mRNA levels were analyzed by quantitative reverse-transcription polymerase chain reaction or ISH, GRP78 expression was increased in patients with UAP ($P=0.14$; Figure 2D), whereas CHOP expression was significantly higher in UAP patients than in SAP patients ($P<0.05$; Figure 2E). On the other hand, both GRP78 and CHOP were significantly increased according to ISH (Figure 2F), but we could not confirm a significant increase of GRP78 by reverse-transcription polymerase chain reaction. This may have been because the number of fresh DCA specimens was too low.

Immunohistochemical Detection of 7-KC in the Fibrous Caps of Atherosclerotic Plaques

To explore the likely molecular mechanism of activation of ER stress and the mechanistic link to apoptosis, we investigated plaque lipids by staining frozen coronary artery sections with anti-7-KC antibody (Figure 3), and the in vitro studies were performed (Figure 4). Immunoreactivity for 7-KC was increased in the fibrous caps of thin-cap atheroma, whereas no immunoreactivity was detected in the fibrous caps of thick-cap atheroma (Figure 3). In the region around the lipid core, however, 7-KC immunoreactivity was visible in both types of atheroma (Figure 3).

Upregulation of ER Chaperones, CHOP, and Apoptosis by 7-KC and Effects of CHOP Knockdown by siRNA in CASMCs or THP-1 Cells

Exposure of cells to 7-KC increased the expression of GRP78 and CHOP mRNA, whereas this increase was prevented by

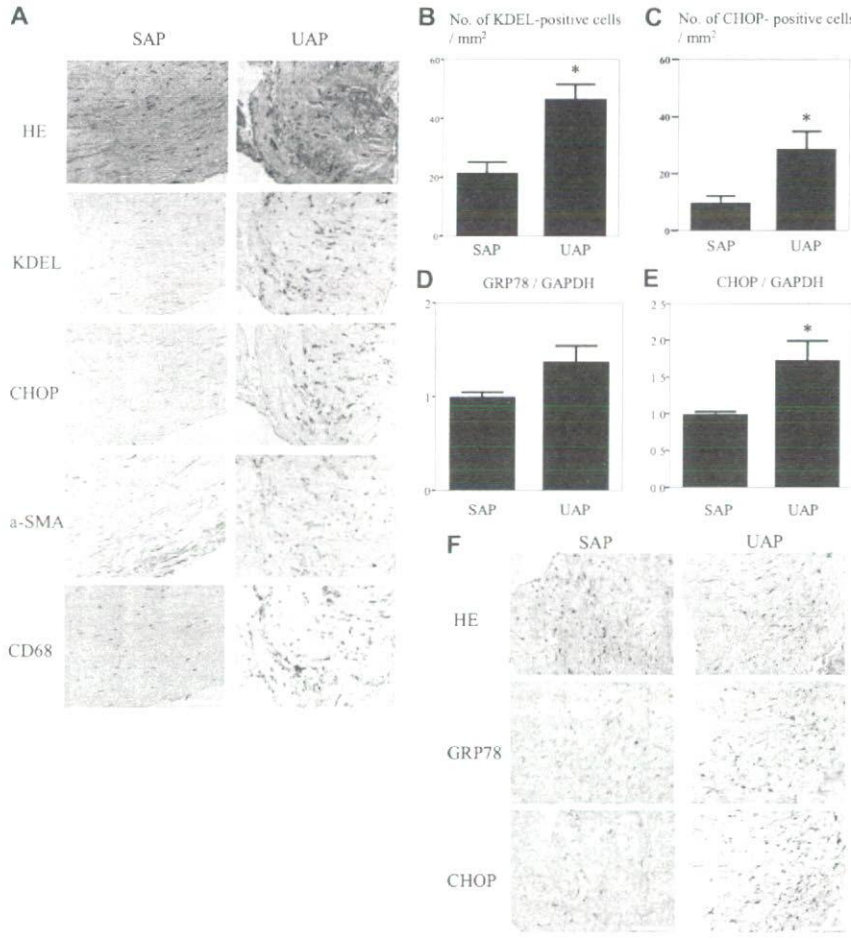

Figure 2. Induction of ER chaperones and death signals in atherectomy specimens obtained from the culprit lesions of patients with UAP. A, Comparison of hematoxylin-eosin (HE) staining with KDEL, CHOP, α-smooth muscle actin (a-SMA), and CD68 immunostaining of the serial sections of 32 atherectomy specimens obtained from patients with SAP (n=16) or UAP (n=16). B and C, Number of KDEL-positive (B) and CHOP-positive (C) cells per square millimeter. D and E, Comparison of GRP78 and CHOP expression normalized for GAPDH in 8 specimens from patients with SAP (n=4) or UAP (n=4) by quantitative reverse-transcription polymerase chain reaction. F, HE staining and ISH analysis of GRP78 (a, d) and CHOP (b, e) mRNA expression in specimens from SAP patients (n=6) or UAP patients (n=6). Scale bar represents 50 μm. *$P<0.05$ vs SAP.

the antioxidants *N*-acetylcysteine or glutathione (Figure 4A). We observed intracellular production of reactive oxygen species after exposure to 7-KC, whereas glutathione reduced reactive oxygen species production (Figure 4B). We also examined the effects of 7-KC on apoptosis of CASMCs and THP-1 cells (Figure 4C). Treatment with 7-KC increased FITC-annexin and propidium iodide staining in a dose-dependent (Figure 4C, b and c) and time-dependent (data not shown) manner. Treatment of CASMCs and THP-1 cells with 7-KC for 24 hours also induced apoptosis along with the induction of ER chaperones and CHOP at the protein level (Figure 4D). When CASMCs and THP-1 cells were simultaneously incubated with 7-KC and *N*-acetylcysteine or glutathione, both antioxidants reduced the induction of ER chaperones (Figure 4D). Quantitative analysis revealed that most of the CHOP-positive cells coexpressed KDEL (88.2% of CHOP-positive CASMCs and 72.7% of CHOP-positive THP-1 cells; $P<0.05$, Fisher's exact test), whereas there were few KDEL-negative and CHOP-positive cells, which suggests that CHOP was involved in the mediation of ER-initiated signaling (Figure 4D, c and d). Treatment of THP-1 cells with 7-KC induced CHOP, whereas 2 different siRNAs targeting CHOP caused the knockdown of CHOP expression (Figure 4E, a). Knockdown of CHOP expression by siRNA decreased the number of TUNEL-positive THP-1 cells after exposure to 7-KC (Figure 4E, b and d). Similarly, the knockdown of CHOP expression by siRNA decreased the number of TUNEL-positive CASMCs after exposure to 7-KC (Figure 4E, c).

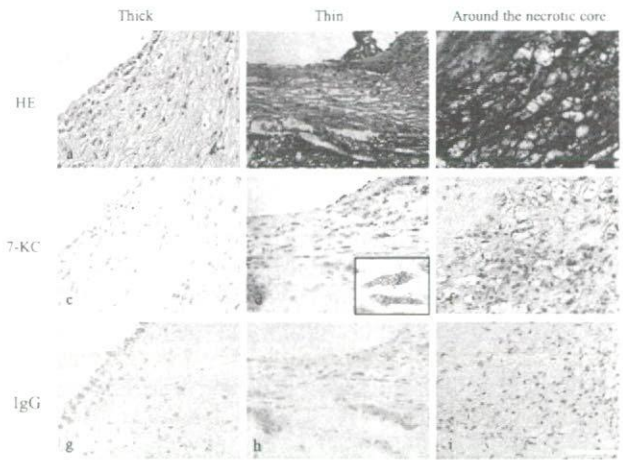

Figure 3. Immunohistochemical detection of 7-KC in the fibrous cap of thin-cap atheroma. Comparison of hematoxylin-eosin (HE) staining with 7-KC or IgG immunostaining in the fibrous caps of thick-cap atheroma (n=6) and thin-cap atheroma (n=6), as well as around the necrotic core of thick-cap atheroma. 7-KC immunostaining is shown at a higher magnification in the inset. Scale bar represents 50 μm.

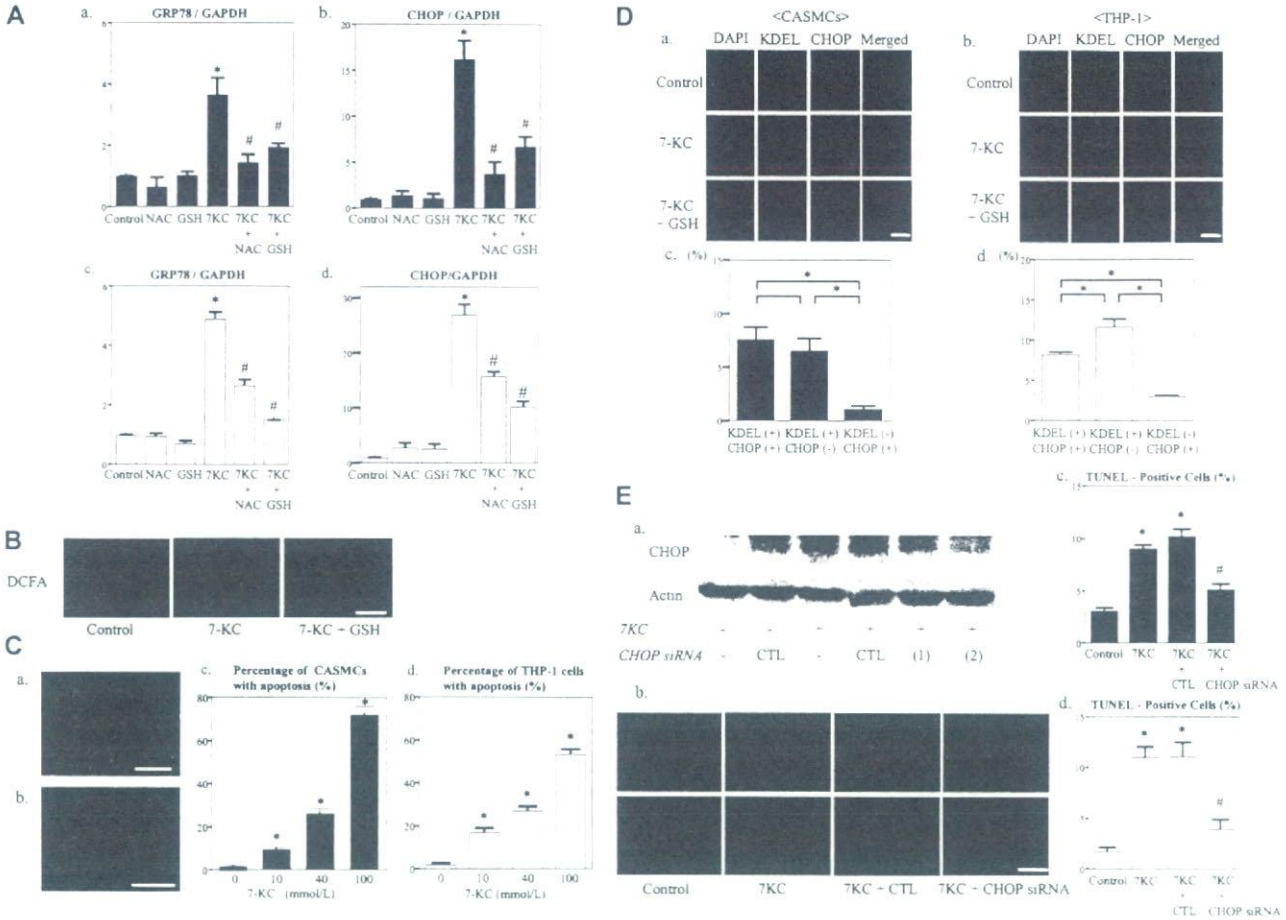

Figure 4. Upregulation of ER chaperones, CHOP, and apoptosis by exposure to 7-KC and effect of CHOP knockdown by siRNA in cultured CASMCs or THP-1 cells. A, Comparison of GRP78 and CHOP expression normalized for GAPDH by quantitative reverse-transcription polymerase chain reaction. CASMCs or THP-1 cells were incubated with 7-KC (80 mmol/L) in the absence or presence of *N*-acetylcysteine (NAC) or glutathione (GSH) for 12 hours. B, Measurement of reactive oxygen species (ROS) generation after exposure to 7-KC and 2', 7'-dichlorofluorescin diacetate (DCFH-DA) in the absence or presence of GSH for 12 hours. C, FITC-annexin V and propidium iodide staining for apoptosis of CASMCs and THP-1 cells incubated with 7-KC (a). Exposure to 7-KC induced apoptosis of CASMCs (b) and THP-1 cells (c) in a dose-dependent manner. D, KDEL and CHOP staining of CASMCs (a) and THP-1 cells (b) after incubation with 7-KC in the absence or presence of GSH for 24 hours; c and d, quantitative analysis of immunohistochemical staining of CASMCs (c) and THP-1 cells (d). E, Western blotting for CHOP after exposure to 7-KC with or without CHOP siRNA (a). TUNEL staining of THP-1 cells (b) and quantitative analysis of TUNEL-positive CASMCs (c) and THP-1 cells (d). CTL indicates the nonsilenced control. Scale bars represent 50 μm (B, C, and E) and 20 μm (D). *$P<0.05$ vs control (A, C, and E). #$P<0.05$ vs treatment with 7-KC (E). Experiments were performed at least 3 times. The data are expressed as mean±SEM. The immunofluorescent staining and Western blotting data are representative of at least 3 independent experiments.

Discussion

The present study revealed a marked increase of ER chaperone expression, CHOP expression, and apoptosis in the fibrous caps of thin-cap atheroma or ruptured plaques, as well as in atherectomy specimens from UAP patients, which suggests that ER stress may play a role in the progression of plaque vulnerability and the occurrence of acute complications of coronary atherosclerosis in humans. Because of the inherent limitations of an autopsy study, we could not exclude the possibility that UPR activation occurred after plaque rupture. Previous reports have shown that ER chaperones, such as GRP78 or GRP94, may have a protective effect against ischemia/reperfusion injury.[34] However, the presence of apoptotic changes in the thin-cap atheroma of the patients with noncardiac death suggested that the findings we observed in ruptured plaques represented the evolution of such changes in the thin-cap atheroma rather than being secondary to plaque rupture or ischemia/reperfusion injury. Only specimens from patients without percutaneous coronary intervention were studied, to exclude the influence of this intervention. We also observed an increase of ER stress-related changes in freshly fixed atherectomy specimens obtained from UAP patients compared with those from SAP patients. This suggests that ER stress activation was related to the clinical situation, and the autopsy specimens were only slightly affected by postmortem protein degradation.

Among the oxysterols, 7-KC is most frequently detected at high levels in atherosclerotic plaques and in the plasma of patients with a high cardiovascular risk.[26,35] To the best of our knowledge, however, 7-KC has not previously been detected in human atherosclerotic coronary artery sections by immunohistochemistry. It has been reported that 7-KC induces the

production of reactive oxygen species, activation of the UPR, and induction of apoptotic death in cultured human SMCs.[28] We demonstrated that the fibrous caps of thin-cap atheroma were immunohistochemically positive for 7-KC, a finding consistent with the increase of ER stress/UPR markers.

Treatment of CASMCs with 7-KC induced ER stress and activation of the UPR, findings that were consistent with the results of a previous study on aortic SMCs,[28] and these changes also occurred in THP-1 cells. This 7-KC–induced cellular damage was prevented by antioxidants (*N*-acetylcysteine and glutathione), which was also consistent with a previous report.[36] Accordingly, the present findings suggest that an increase of ER stress due to 7-KC induces apoptosis of SMCs and macrophages through the production of reactive oxygen species.

ER stress induces apoptosis via the CHOP-, JNK-, and caspase-12–dependent signaling pathways.[16] CHOP is mainly induced at the transcriptional level by ER stress,[12,37] after which its overexpression leads to apoptosis.[11,16,38] CHOP knockout mice show normal development and normal fertility but exhibit less apoptosis in response to ER stress.[16,21] Thus, detection of the induction of CHOP indicates an increase of ER-initiated apoptosis. Although the direct transcriptional target of CHOP has not been found,[39] the Bcl-2 pathway may be involved in the downstream connection between CHOP and apoptosis.[28,39] Caspase-12 is only activated by ER stress.[13,16,18] Although caspase-12 has been cloned in mice and rats, it is not yet possible to explore the role of this caspase in humans.[40] JNK is 1 of the stress-activated protein kinases that has been shown to induce apoptosis in response to ER stress.[13,16] We demonstrated that TUNEL-positive SMCs and macrophages were significantly increased in the fibrous cap, with CHOP (but not JNK) being induced simultaneously. Treatment of CASMCs or THP-1 cells with 7-KC induced CHOP, whereas knockdown of CHOP expression by siRNA led to a decrease of TUNEL-positive cells after exposure to 7-KC. Because CHOP is a transcription factor that specifically mediates ER-initiated apoptosis, the induction of CHOP in ruptured and unstable plaques supports the activation of ER-initiated apoptosis. However, our autopsy study could not exclude the possibility that the cells underwent apoptosis independently of CHOP, whereas the TUNEL assay gave false-positive results in the clinical specimens.

Unfortunately, we could not confirm whether or not the relationship between thinning of the fibrous cap and ER stress was causative because of the lack of a suitable animal model of plaque rupture. On the other hand, together with the present finding that 7-KC induced ER stress, the possibility that ER stress causes plaque vulnerability is also supported by the following reports. In cultured peritoneal macrophages, excessive accumulation of free cholesterol has been found to initiate ER stress, increase CHOP expression, and increase apoptosis.[21] Moreover, in vivo studies with apoE$^{-/-}$ mice have shown that lesional necrosis can be diminished by a decrease in the cholesterol level.[22] In addition, the present study demonstrated that expression of ER chaperones was upregulated to a similar extent in macrophages surrounding the necrotic cores of thick-cap atheroma, thin-cap atheroma, and ruptured plaques, which suggests that ER stress may contribute to the progression of plaque vulnerability by inducing macrophage apoptosis.

In conclusion, the present findings support the possibility that ER stress and/or the UPR induces apoptosis of SMCs and macrophages, thus increasing the vulnerability of coronary artery plaques, which may lead to ACS and a fatal outcome in patients with coronary artery disease.

Acknowledgments

We thank Akiko Ogai, Tomoko Morita, and Kazuyoshi Masuda for their technical assistance and Akiko Kada and Nobuo Shirahashi for their statistical advice.

Sources of Funding

The present study was supported by a grant from the Japan Cardiovascular Research Foundation and a research grant for cardiovascular disease (14C-4) from the Japanese Ministry of Health, Labor and Welfare.

Disclosures

None.

References

1. Fuster V, Lewis A, Conner Memorial Lecture: mechanisms leading to myocardial infarction: insights from studies of vascular biology. *Circulation*. 1994;90:2126–2146.
2. Lee RT, Libby P. The unstable atheroma. *Arterioscler Thromb Vasc Biol*. 1997;17:1859–1867.
3. Falk E, Shah PK, Fuster V. Coronary plaque disruption. *Circulation*. 1995;92:657–671.
4. Bennett MR. Apoptosis of vascular smooth muscle cells in vascular remodeling and atherosclerotic plaque rupture. *Cardiovasc Res*. 1999;41:361–368.
5. Bjorkerud S, Bjorkerud B. Apoptosis is abundant in human atherosclerotic lesions, especially in inflammatory cells (macrophages and T cells), and may contribute to the accumulation of gruel and plaque instability. *Am J Pathol*. 1996;149:367–380.
6. Littlewood TD, Bennett MR. Apoptotic cell death in atherosclerosis. *Curr Opin Lipidol*. 2003;14:469–475.
7. Lindstedt KA, Leskinen MJ, Kovanen PT. Proteolysis of the pericellular matrix: a novel element determining cell survival and death in the pathogenesis of plaque erosion and rupture. *Arterioscler Thromb Vasc Biol*. 2004;24:1350–1358.
8. Kockx MM, De Meyer GR, Muhring J, Jacob W, Bult H, Herman AG. Apoptosis and related proteins in different stages of human atherosclerotic plaques. *Circulation*. 1998;97:2307–2315.
9. Kolodgie FD, Narula J, Burke AP, Haider N, Farb A, Hui-Liang Y, Smialek J, Virmani R. Localization of apoptotic macrophages at the site of plaque rupture in sudden coronary death. *Am J Pathol*. 2000;157:1259–1268.
10. Stoneman V, Bennet MR. Role of apoptosis in atherosclerosis and its therapeutic implications. *Clin Sci*. 2004;107:343–354.
11. Kaufman RJ. Stress signaling from the lumen of the endoplasmic reticulum: coordination of gene transcriptional and translational controls. *Genes Dev*. 1999;13:1211–1233.
12. Ron D. Translational control in the endoplasmic reticulum stress response. *J Clin Invest*. 2002;110:1383–1388.
13. Ferri KF, Kroemer G. Organelle-specific initiation of cell death pathways. *Nat Cell Biol*. 2001;3:E255–E263.
14. Patterson C, Cyr D. Welcome to the machine: a cardiologist's introduction to protein folding and degradation. *Circulation*. 2002;106:2741–2746.
15. Mori K. Tripartite management of unfolded proteins in the endoplasmic reticulum. *Cell*. 2000;101:451–454.
16. Oyadomari S, Araki E, Mori M. Endoplasmic reticulum stress-mediated apoptosis in pancreatic beta-cells. *Apoptosis*. 2002;7:335–345.
17. Okada K, Minamino T, Tsukamoto Y, Liao Y, Tsukamoto O, Takashima S, Hirata A, Fujita M, Nagamachi Y, Nakatani T, Yutani C, Ozawa K, Ogawa S, Tomoike H, Hori M, Kitakaze M. Prolonged endoplasmic

reticulum stress in hypertrophic and failing heart after aortic constriction. *Circulation*. 2004;110:705–712.
18. Nakagawa T, Zhu H, Morishima N, Li E, Xu J, Yankner BA, Yuan J. Caspase-12 mediates endoplasmic-reticulum-specific apoptosis and cytotoxicity by amyloid-beta. *Nature*. 2000;403:98–103.
19. Little E, Tocco G, Baudry M, Lee AS, Schreiber SS. Induction of glucose-regulated protein (glucose-regulated protein 78/BiP and glucose-regulated protein 94) and heat shock protein 70 transcripts in the immature rat brain following status epilepticus. *Neuroscience*. 1996;75:209–219.
20. Ross R. Atherosclerosis: an inflammatory disease. *N Engl J Med*. 1999;340:115–126.
21. Feng B, Yao PM, Li Y, Devlin CM, Zhang D, Harding HP, Sweeney M, Rong JX, Kuriakose G, Fisher EA, Marks AR, Ron D, Tabas I. The endoplasmic reticulum is the site of cholesterol-induced cytotoxicity in macrophages. *Nat Cell Biol*. 2003;5:781–792.
22. Feng B, Zhang D, Kuriakose G, Devlin CM, Kockx M, Tabas I. Niemann-Pick C heterozygosity confers resistance to lesional necrosis and macrophage apoptosis in murine atherosclerosis. *Proc Natl Acad Sci U S A*. 2003;100:10423–10428.
23. Zhou J, Lhoták S, Hilditch BA, Austin RC. Activation of unfolded protein response occurs at all stages of atherosclerotic lesion development in apolipoprotein E-deficient mice. *Circulation*. 2005;111:1814–1821.
24. Cullen P, Baetta R, Bellosta S, Bernini F, Chinetti G, Cignarella A, von Eckardstein A, Exley A, Goddard M, Hofker M, Hurt-Camejo E, Kanters E, Kovanen P, Lorkowski S, McPheat W, Pentikainen M, Rauterberg J, Ritchie A, Staels B, Weitkamp B, de Winther M; for the MAFAPS Consortium. Rupture of the atherosclerotic plaque: does a good animal model exist? *Arterioscler Thromb Vasc Biol*. 2003;23:535–542.
25. Lutgens E, Suylen R, Faber BC, Gijbels MJ, Eurlings PM, Bijnens AP, Cleutjens KB, Heeneman S, Daemen MJ. Atherosclerotic plaque rupture: local or systemic process? *Arterioscler Thromb Vasc Biol*. 2003;23:2123–2130.
26. Brown AJ, Jessup W. Oxysterols and atherosclerosis. *Atherosclerosis*. 1999;142:1–28.
27. Bjorkhem I, Diczfalusy U. Oxysterols: friends, foes, or just fellow passengers? *Arterioscler Thromb Vasc Biol*. 2002;22:734–742.
28. Pedruzzi E, Guichard C, Ollivier V, Driss F, Fay M, Prunet C, Marie JC, Pouzet C, Samadi M, Elbim C, O'Dowd Y, Bens M, Vandewalle A, Gougerot-Pocidalo MA, Lizard G, Ogier-Denis E. NAD(P)H oxidase Nox-4 mediates 7-ketocholesterol-induced endoplasmic reticulum stress and apoptosis in human aortic smooth muscle cells. *Mol Cell Biol*. 2004;24:10703–10717.
29. Naruko T, Ueda M, Haze K, van der Wal AC, van der Loos CM, Itoh A, Komatsu R, Ikura Y, Ogami M, Shimada Y, Ehara S, Yoshiyama M, Takeuchi K, Yoshikawa J, Becker AE. Neutrophil infiltration of culprit lesions in acute coronary syndromes. *Circulation*. 2002;106:2894–2900.
30. Stary HC, Chandler AB, Glagov S, Guyton JR, Insull W Jr, Rosenfeld ME, Schaffer A, Schwartz CJ, Wagner WD, Wissler RW. A definition of initial, fatty streak, and intermediate lesions of atherosclerosis. *Arterioscler Thromb*. 1994;14:840–856.
31. Stary HC, Chandler AB, Dinsmore RE, Fuster V, Glagov S, Insull W, Rosenfeld ME, Schwartz CJ, Wagner WD, Wissler RW. A definition of advanced types of atherosclerotic lesions and a histological classification of atherosclerosis. *Arterioscler Thromb Vasc Biol*. 1995;15:1512–1531.
32. Kolodgie FD, Burke AP, Farb A, Gold HK, Yuan J, Narula J, Finn AV, Virmani R. The thin-cap fibroatheroma: a type of vulnerable plaque: the major precursor lesion to acute coronary syndromes. *Curr Opin Cardiol*. 2001;16:285–292.
33. Kuniyasu H, Ukai R, Johnston D, Troncoso P, Fidler IJ, Pettaway CA. The relative mRNA expression levels of matrix metalloproteinase to E-cadherin in prostate biopsy specimens distinguishes organ-confined from advanced prostate cancer at radical prostatectomy. *Clin Cancer Res*. 2003;9:2185–2194.
34. Martindale JJ, Fernandez R, Thuerauf D, Whittaker R, Gude N, Sussman MA, Glembotski CC. Endoplasmic reticulum stress gene induction and protection from ischemia/reperfusion injury in the hearts of transgenic mice with a tamoxifen-regulated form of ATF6. *Circ Res*. 2006;98:1186–1193.
35. Zhou Q, Wasowicz E, Handler B, Fleischer L, Kummerow FA. An excess concentration of oxysterols in the plasma is cytotoxic to cultured endothelial cells. *Atherosclerosis*. 2000;149:191–197.
36. Lizard G, Gueldry S, Sordet O, Monier S, Athias A, Miguet C, Bessede G, Lemaire S, Solary E, Gambert P. Glutathione is implied in the control of 7-ketocholesterol-induced apoptosis, which is associated with radical oxygen species production. *FASEB J*. 1998;12:1651–1663.
37. Wang XZ, Lawson B, Brewer JW, Zinszner H, Sanjay A, Mi LJ, Boorstein R, Kreibich G, Hendershot LM, Ron D. Signals from the stressed endoplasmic reticulum induce C/EBP-homologous protein (CHOP/GADD153). *Mol Cell Biol*. 1996;16:4273–4280.
38. Barone MV, Crozat A, Tabaee A, Philipson L, Ron D. CHOP (GADD153) and its oncogenic variant, TLSCHOP, have opposing effects on the induction of G1/S arrest. *Genes Dev*. 1994;8:453–464.
39. Oyadomari S, Mori M. Roles of CHOP/GADD153 in endoplasmic reticulum stress. *Cell Death Differ*. 2004;11:381–389.
40. Fischer H, Koenig U, Eckhart L, Tschachler E. Human caspase 12 has acquired deleterious mutations. *Biochem Biophys Res Commun*. 2002;293:722–772.

CLINICAL PERSPECTIVE

Most of the acute clinical manifestations of coronary atherosclerosis result from plaque rupture that produces the acute coronary syndrome, and apoptosis is considered to be essential for plaque rupture. The endoplasmic reticulum (ER) is 1 of the largest cellular organelles and has multiple functions, such as regulating the folding of proteins. Various stimuli cause ER stress, including ischemia, heat shock, mutation, increased protein synthesis, and reactive oxygen species, all of which can potentially lead to ER dysfunction. The ER responds to stresses by upregulation of ER chaperones, but prolonged ER stress eventually causes apoptosis. However, the influence of ER stress and apoptosis on rupture of unstable coronary plaques remains unclear. We examined histological sections from coronary artery segments obtained at autopsy from 71 patients and atherectomy specimens obtained from 40 patients. Smooth muscle cells and macrophages in the fibrous caps of thin-cap atheroma and ruptured plaques showed a marked increase of ER chaperone expression and apoptotic cells. ER chaperones also showed higher expression in atherectomy specimens from patients with unstable angina pectoris than from those with stable angina. We also investigated possible signaling pathways for ER-initiated apoptosis and found that the C/EBP homologous protein (a transcription factor induced by ER stress)–dependent pathway was activated in unstable plaques. In addition, knockdown of C/EBP homologous protein expression by small interfering RNA decreased ER stress-dependent death of cultured coronary artery smooth muscle cells and THP-1 cells. Increased ER stress occurs in unstable plaques. Our findings suggest that ER stress-induced apoptosis may contribute to plaque vulnerability.

A cardiac myosin light chain kinase regulates sarcomere assembly in the vertebrate heart

Osamu Seguchi,[1] Seiji Takashima,[2,3] Satoru Yamazaki,[1] Masanori Asakura,[1] Yoshihiro Asano,[2] Yasunori Shintani,[2] Masakatsu Wakeno,[1] Tetsuo Minamino,[2] Hiroya Kondo,[2] Hidehiko Furukawa,[4] Kenji Nakamaru,[4] Asuka Naito,[4] Tomoko Takahashi,[4] Toshiaki Ohtsuka,[4] Koichi Kawakami,[5] Tadashi Isomura,[6] Soichiro Kitamura,[1] Hitonobu Tomoike,[1] Naoki Mochizuki,[1] and Masafumi Kitakaze[1]

[1]Department of Cardiovascular Medicine, National Cardiovascular Center, Suita, Osaka, Japan. [2]Department of Cardiovascular Medicine and [3]Health Care Center, Osaka University Graduate School of Medicine, Suita, Osaka, Japan. [4]Core Technology Research Laboratories, Sankyo Co. Ltd., Shinagawa, Tokyo, Japan. [5]Division of Molecular and Developmental Biology, National Institute of Genetics, Mishima, Shizuoka, Japan. [6]Hayama Heart Center, Hayama, Kanagawa, Japan.

Marked sarcomere disorganization is a well-documented characteristic of cardiomyocytes in the failing human myocardium. Myosin regulatory light chain 2, ventricular/cardiac muscle isoform (MLC2v), which is involved in the development of human cardiomyopathy, is an important structural protein that affects physiologic cardiac sarcomere formation and heart development. Integrated cDNA expression analysis of failing human myocardia uncovered a novel protein kinase, cardiac-specific myosin light chain kinase (cardiac-MLCK), which acts on MLC2v. Expression levels of cardiac-MLCK were well correlated with the pulmonary arterial pressure of patients with heart failure. In cultured cardiomyocytes, knockdown of cardiac-MLCK by specific siRNAs decreased MLC2v phosphorylation and impaired epinephrine-induced activation of sarcomere reassembly. To further clarify the physiologic roles of cardiac-MLCK in vivo, we cloned the zebrafish ortholog z-cardiac-MLCK. Knockdown of z-cardiac-MLCK expression using morpholino antisense oligonucleotides resulted in dilated cardiac ventricles and immature sarcomere structures. These results suggest a significant role for cardiac-MLCK in cardiogenesis.

Introduction

Despite recent advances in pharmacologic and surgical therapies, chronic heart failure (CHF) is still a leading cause of death worldwide (1). Currently, heart transplant is thought to be the most effective therapy for end-stage CHF. However, this approach obviously cannot be used for all of the numerous affected patients and is not suitable for patients with a mild disease state. Therefore, there is increasing demand for new therapeutic targets for CHF.

Cardiomyocytes, the most basic cellular unit of the myocardium, express several sarcomeric proteins, including myosin and actin; abnormalities in these sarcomeric proteins are major causes of idiopathic cardiomyopathies and lead to CHF (2–4). Type II myosin is the major constituent of sarcomeres. In the neck region of this protein, there are binding sites for a pair of myosin light chains, which are called the essential light chain and the regulatory light chain. Among the several paralogs of the myosin regulatory light chain in vertebrates (5), myosin regulatory light chain 2, ventricular/cardiac muscle isoform (MLC2v) is expressed in the myocardium, where it performs specific roles in cardiogenesis by contributing to the formation of sarcomeres and in increasing the Ca^{2+} sensitivity of muscle tension at submaximal Ca^{2+} concentrations (6, 7). Currently, 2 members of the myosin light chain kinase (MLCK) protein family that act on myosin regulatory light chain in muscle cells have been identified, skeletal muscle MLCK (skMLCK) and smooth muscle MLCK (smMLCK) (8). Among these MLCK family members, smMLCK, including nonmuscle isoforms, is distributed ubiquitously in various tissues and contributes to the contraction of smooth muscle and several cell activities. Conversely, skMLCK is thought to localize and function in both cardiac muscle and skeletal muscle (9); to our knowledge, no cardiac-specific MLCK has been reported to date. skMLCK-deficient mice, however, did not show any heart weight, body weight, or heart weight/body weight ratio phenotypes, despite effective knockdown of skMLCK expression (10). Additionally, there were no significant differences between the knockout and wild-type animals in regard to MLC2v phosphorylation, suggesting the existence of as-yet unknown kinases in cardiac muscle cells.

Genome-wide analyses, which have recently become available in a wide range of clinical settings, such as cancer research, allow for a global view of gene expression in certain disease states and the identification of unknown molecules and molecular pathways that can be exploited as novel therapeutic targets. CHF is a candidate disease for this type of genome-wide analysis, because of its heterogeneous properties and previous difficulties identifying responsible genes using other conventional modalities.

In this study, we performed microarray analysis of the failing human myocardium and examined the correlation between the obtained genomic data and the clinical, physiological, and biochemical characteristics of CHF. In this manner, we sought to identify candidate genes that are involved in the pathophysiology of CHF. Consequently, we identified what we believe to be a novel

Nonstandard abbreviations used: ANP, atrial natriuretic peptide; BNP, brain natriuretic peptide; CHF, chronic heart failure; cardiac-MLCK, cardiac-specific MLCK; Dd, end-diastolic dimension; Ds, end-systolic dimension; FS, fractional shortening; hpf, hours postfertilization; MI, myocardial infarction; MLC2v, myosin regulatory light chain 2, ventricular/cardiac muscle isoform; MLCK, myosin light chain kinase; M-mode, motion mode; MO, morpholino antisense oligonucleotide; p-s15MLC, antibodies for phosphorylated MLC2v; PAP, pulmonary arterial pressure; RcMK, antibodies specific for rodent cardiac-MLCK; si-cMK, siRNA targeting cardiac-MLCK; si-smMK, siRNA targeting rat smMLCK; skMLCK, skeletal muscle MLCK; smMLCK, smooth muscle MLCK; tMLC, antibodies for total MLC2v; z-, zebrafish; z-cMKaugMO, MO targeting the AUG translational start site of z-cardiac-MLCK.

Conflict of interest: The authors have declared that no conflict of interest exists.

Citation for this article: *J. Clin. Invest.* **117**:2812–2824 (2007). doi:10.1172/JCI30804.

Table 1
Clinical characteristics of the patients used for microarray analysis

Pt	Age (yr)	Sex	Diagnosis	Operation	Dd (mm)	EF (%)	PAP (mmHg)	ANP (pg/ml)	BNP (pg/ml)
1	53	M	DCM, MI	Batista	88	25	20	25	90.4
2	45	M	DCM	Batista	81	39	45	85	217
3	72	M	DCM	Batista	71	14	25	86	201
4	58	M	MI	Dor	76	–	–	–	–
5	57	M	HCM, MI	Dor	52	44	41	20	80.3
6	69	M	DCM	Batista	86	19	59	100	465
7	40	M	AR	Unknown	76	42	16	52	271
8	75	M	MI	Dor	51	55	–	39	174
9	32	M	DCM	Batista	81	26	26	300	869
10	51	F	Sarcoidosis	Dor	68	35	–	89	339
11	54	M	MI	Dor	63	37	–	84	302
12	58	M	Myocarditis	Dor	77	22	–	800	2,710
N-1	27	M	Normal	–	–	–	–	–	–
N-2	24	M	Normal	–	–	–	–	–	–

AR, aortic regurgitation; DCM, dilated cardiomyopathy; EF, ejection fraction; F, female; HCM, hypertrophic cardiomyopathy; M, male; Pt, patient.

cardiac-specific MLCK (cardiac-MLCK; encoded by *MYLK3*). Phosphorylation of MLC2v by cardiac-MLCK regulated the reassembly of sarcomere structures in cultured neonatal rat cardiomyocytes. Suppression of cardiac-MLCK expression in zebrafish embryos using specific morpholino antisense oligonucleotides (MOs) led to dilation of the cardiac ventricle with incomplete sarcomere formation, suggesting critical roles for cardiac-MLCK in the heart.

Results

Identification of cardiac-MLCK from failing human myocardia using microarray analysis. To identify candidate genes involved in the pathophysiology of CHF, we used an HG-U95 Affymetrix GeneChip to analyze the gene expression profiles of failing myocardial tissues obtained from 12 patients who had undergone cardiac exclusion surgery, such as the Dor or Batista procedures, for end-stage CHF (Table 1). Figure 1A is an overview flowchart for the selection of candidate genes. Compared with those of 2 normal control samples, the expression of 626 probe sets was significantly upregulated in the failing myocardia. Of these, we selected probe sets whose expression levels were positively correlated ($r > 0.7$) with pulmonary arterial pressure (PAP) measurements (129 probe sets) and brain natriuretic peptide (BNP) mRNA levels (194 probe sets). The tissue localization of each selected probe set was then analyzed using the commercially available BioExpress database (Gene Logic Inc.). We selected 10 probe sets, for which the cardiac expression level was at least 10-fold the mean expression level of 24 other tissues, for further analysis. These probe sets represented a set of genes that included atrial natriuretic peptide (ANP), BNP, small muscle protein, and α-actin, all of which are known to be involved in heart failure, cardiac muscle remodeling, and striated muscle function. We calculated the ratios of expression in cardiac muscle to that in skeletal muscle in these probe sets. ANP (36663_at and 73106_s_at), BNP (39215_at), Importin9 (84730_at), and 75678_at exhibited expression levels that were at least 10-fold greater in the heart than in skeletal muscle. Expression levels of 75678_at, for which annotation was not available, were similar to those of ANP and BNP. We hypothesized that this unknown transcript was involved in the pathophysiology of heart failure.

Using 5′-RACE, we identified specific sequences identical to those of NM_182493 (*MYLK3*) located 4 kb upstream of the probe set sequence. The relative expression level of this candidate gene was significantly correlated with the relative PAP value (Figure 1B); in addition, the expression of this gene was restricted to the heart (Figure 1C). A homology search using the transcript sequence, particularly the sequence coding for the C-terminal kinase domain, identified *MYLK3* as a member of the MLCK family. Thus, we named the protein encoded by *MYLK3* "cardiac-MLCK." Two distinct MLCK family genes have been previously reported: *MYLK*, which encodes smMLCK, and *MYLK2*, which encodes skMLCK (8). Domain structure analysis revealed a well-conserved serine/threonine kinase domain that includes an ATP-binding site and an active serine/threonine kinase domain positioned near the C terminus of the cardiac-MLCK protein (Figure 1D). The expression patterns of the MLCK family members were confirmed by Northern blot analysis. As previously described (11), 2 major transcripts of *MYLK* were almost ubiquitously expressed. The larger transcript codes for a nonmuscle isoform of smMLCK generated by alternative splicing. Restricted expression patterns were observed for both *MYLK2* and *MYLK3*. *MYLK2* expression was only detected in skeletal muscle, whereas *MYLK3* expression was only observed in the heart (Figure 1E). *MYLK* was also found to be expressed in the heart, although its expression was not upregulated in failing myocardia as much as the expression of *MYLK3* (data not shown). To assess the physiological significance of cardiac-MLCK, we generated an adenovirus vector encoding cardiac-MLCK. In serum-free conditions, cultured neonatal rat cardiomyocytes showed predominantly disorganized sarcomere structures. Overexpression of cardiac-MLCK in cultured neonatal rat cardiomyocytes augmented sarcomere organization under serum-starved conditions (cells with organized sarcomeres, 28.7% ± 11.1% versus 3.1% ± 2.4%; $P < 0.001$; Figure 1, F and G), suggesting that cardiac-MLCK participates in sarcomere formation in cardiomyocytes.

Cardiac-specific myosin regulatory light chain is a specific substrate of cardiac-MLCK. Because this protein kinase contained a consensus kinase catalytic domain, we attempted to identify potential substrates of cardiac-MLCK. To identify physiological substrates of cardiac-MLCK, we screened murine heart homogenates using an in vitro kinase reaction. After fractionation of murine heart homogenates using a cation exchange column, aliquots of each fraction were subjected to an in vitro kinase reaction with recombinant cardiac-MLCK. Fractions 10 and 11 each contained a distinct 20-kDa band that was labeled with ^{32}P only in the presence of recombinant cardiac-MLCK (Figure 2A). This ^{32}P-labeled 20-kDa protein was purified (Figure 2B) and analyzed using matrix-assisted laser desorption/ionization-time-of-flight mass spectrometry and peptide mass fingerprinting. The 20-kDa protein contained fragments with amino acid sequences that were homologous to murine MLC2v (Figure 2C). No additional ^{32}P-labeled proteins were detected in fractions obtained following cation or anion exchange column purification. Further analysis of this phosphorylation event in vitro revealed endogenous MLC2v, purified from murine heart homogenates, was phosphorylated by recombinant cardiac-MLCK in a Ca^{2+}-calmodulin–dependent manner (Figure 2D). Thus, we conclude that cardiac-MLCK is a calmodulin-dependent kinase.

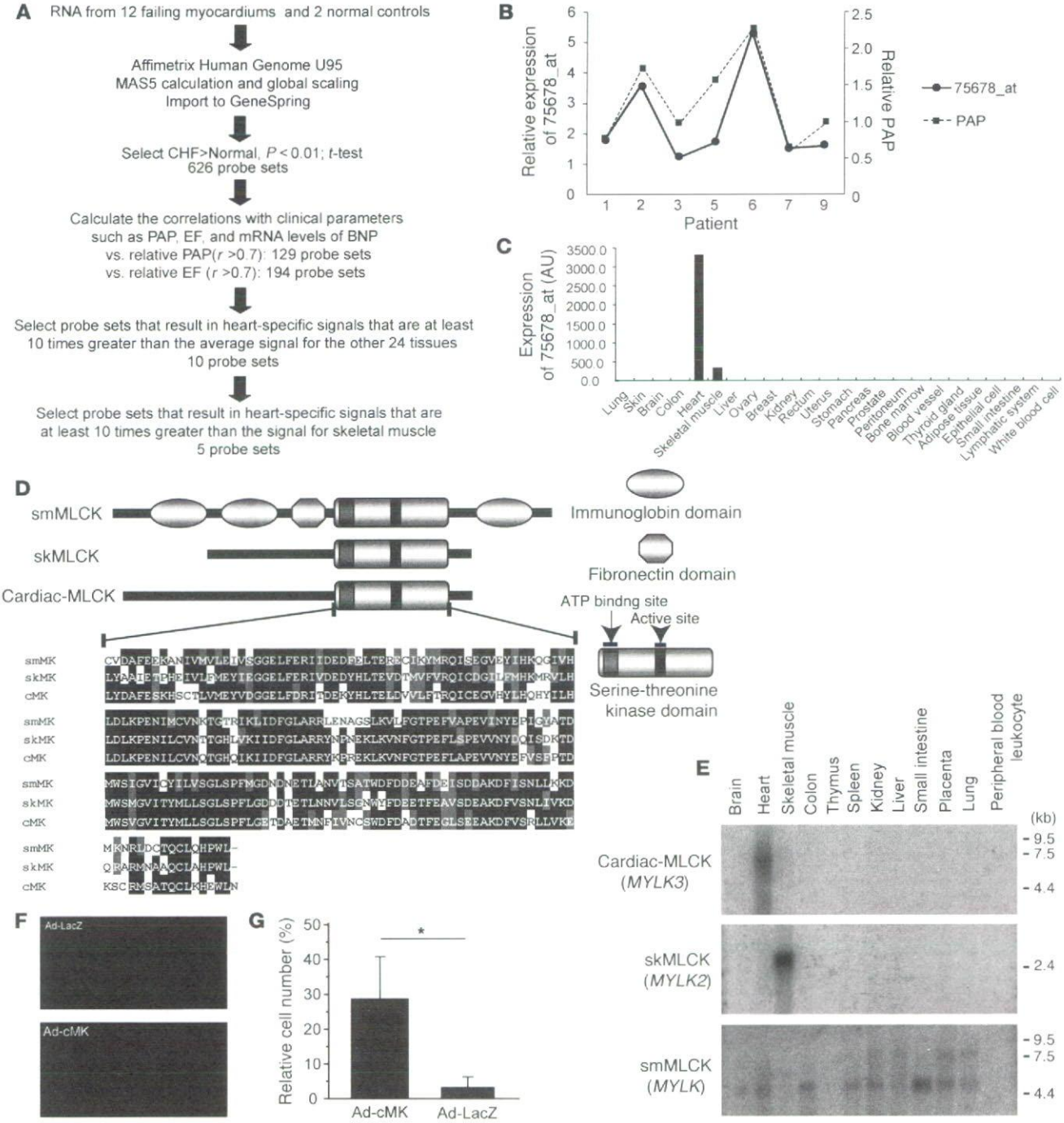

Figure 1

Microarray analysis for candidate gene selection. (**A**) Flowchart for the selection of candidate genes. (**B**) The relative expression levels of 75678_at correlated well with the relative PAP values in the respective patients. (**C**) Tissue localization of the candidate gene expression was analyzed using the GeneExpress database; 75678_at was specifically expressed in the heart. (**D**) Each MLCK family member possesses a highly conserved serine-threonine kinase domain in the C-terminal region of the protein. Amino acid residues on black backgrounds are the most commonly conserved residues at each position; residues on gray backgrounds are similar to the consensus amino acids. (**E**) Expression analysis of MLCK family members using multiple human tissue Northern blot membranes. The 2 transcripts transcribed from *MYLK* (encoding smMLCK) were ubiquitously expressed with the exception of skeletal muscle, thymus, and peripheral blood leukocytes. In contrast, *MYLK2* (encoding skMLCK) and *MYLK3* (encoding cardiac-MLCK) were only expressed in skeletal muscle and heart, respectively. (**F**) Fluorescence microscopy of cardiomyocytes cultured in serum-free conditions and infected with adenovirus encoding LacZ (Ad-LacZ) revealed predominantly round-shaped cells with disorganized sarcomere structures. Infection with adenovirus encoding cardiac-MLCK (Ad-cMK) at a MOI of 120 increased the number of the cells with organized sarcomere structures. Original magnification, ×1,000. (**G**) The percentage of cells with organized sarcomeres was significantly higher in cardiomyocytes infected with adenovirus encoding cardiac-MLCK than in those infected with adenovirus encoding LacZ. Values are mean ± SEM. $^*P < 0.001$.

Next, we generated polyclonal antibodies specific for rodent cardiac-MLCK (RcMK). Antibodies that detected phosphorylated MLC2v (p-s15MLC; anti-rodent serine 15 phosphorylated MLC2v) and total MLC2v (tMLC) were also generated. RcMK detected rat cardiac-MLCK from whole-cell cardiomyocyte extracts as well as recombinant FLAG-tagged murine cardiac-MLCK (Figure 2E). Phosphorylated MLC2v and nonphosphorylated MLC2v could be clearly separated using urea-glycerol gel electrophoresis (12). tMLC detected both phosphorylated and nonphosphorylated MLC2v, whereas p-s15MLC specifically detected the phosphorylated form of MLC2v (Figure 2F). Overexpression of cardiac-MLCK increased the levels of phosphorylated MLC2v in cultured cardiomyocytes (Figure 2G). However, there was no effect on the expression of other sarcomere proteins involved in sarcomere organization such as troponin T, desmin, and α-actinin. mRNA expression of ANP and β myosin heavy chain, representative markers of cardiac hypertrophy, were also unaffected by cardiac-MLCK overexpression (data not shown). To further investigate the phosphorylation of MLC2v by endogenous cardiac-MLCK, we used specific siRNAs targeting cardiac-MLCK (si-cMKs). These siRNAs effectively suppressed the level of cardiac-MLCK mRNA by more than 70%, as determined using quantitative real-time PCR 24 hours after transfection (Figure 2H). These siRNAs also effectively suppressed the level of cardiac-MLCK protein and the amount of phosphorylated MLC2v 60–72 hours after transfection (Figure 2I), whereas no remarkable effects were seen for the expression of other sarcomere proteins. On the contrary, suppression of smMLCK expression, which is also distributed in heart, using siRNA targeting rat smMLCK (si-smMK) did not change either the phosphorylation status of MLC2v or the expression of sarcomere proteins (Figure 2J). These results indicated that cardiac-MLCK predominantly phosphorylates MLC2v, which is selectively expressed in cardiomyocytes. Thus, cardiac-MLCK may regulate morphologic change in cardiomyocytes, including sarcomere organization, through MLC2v phosphorylation.

Cardiac-MLCK regulates sarcomere assembly in cultured cardiomyocytes. To elucidate the precise role of cardiac-MLCK in the sarcomere structure, we analyzed the effects of MLC2v phosphorylation on sarcomeres in cultured neonatal rat cardiomyocytes. Polymerized actin stained with rhodamine-phalloidin revealed a regularly organized pattern of striations (Figure 3A). Phosphorylated MLC2v labeling with p-s15MLC demonstrated a similar striated pattern, although the labeling was predominantly observed in the A-band region, a portion of the sarcomere primarily made up of thick filaments (Figure 3, B–D). Diffuse cytosolic fluorescent labeling was seen when cardiac-MLCK was labeled with RcMK (Figure 3, E–G).

When cardiomyocytes were cultured in serum-free conditions, the organized striation pattern of actin was disrupted and the phosphorylated MLC2v-specific signal decreased (Figure 3K). To evaluate the morphologic changes observed in cardiomyocytes upon activation of endogenous cardiac-MLCK, we treated cardiomyocytes cultured under serum-free conditions with epinephrine. Stimulation of G protein–coupled receptors with epinephrine should activate cardiac-MLCK by increasing intracellular Ca^{2+} concentrations (13). A marked upregulation of MLC2v phosphorylation was obtained following treatment with 2 μM epinephrine (Figure 3H). Epinephrine-induced phosphorylation of MLC2v, which was observed as early as 5 minutes after stimulation, peaked within 30 minutes (Figure 3I). Treatment of the cardiomyocytes cultured in serum-free conditions with 2 μM epinephrine also induced reassembly of sarcomere structures and MLC2v phosphorylation (Figure 3, J, K, and L). To confirm the relevance of MLC2v phosphorylation by cardiac-MLCK, we introduced si-cMKs into cardiomyocytes and analyzed the sarcomere patterns in these cells. The level of phosphorylated MLC2v was reduced 72 hours after transfection with the si-cMKs; however, we did not observe any remarkable changes in the structures of the sarcomeres in cardiomyocytes cultured with serum. The sarcomeres of control siRNA– and si-cMK–treated cells contained organized filament structures (cells with organized sarcomeres, 97.0% ± 1.0% versus 90.0% ± 1.0%; NS; Figure 4, A–F and I). In contrast, the knockdown of cardiac-MLCK produced significant effects on sarcomere reassembly. si-cMK inhibited sarcomere reassembly after epinephrine treatment in cardiomyocytes cultured under serum-free conditions (cells with organized sarcomeres, 76.0% ± 8.5% versus 43.6% ± 7.0%; $P < 0.005$; Figure 4, A–F and I). We also confirmed the phosphorylation of MLC2v using immunoblot analysis (Figure 4G). The results of the immunoblot analysis are quantified in Figure 4H, and the relative MLC2v phosphorylation levels in this experiment exhibited a similar pattern as the percentages of cardiomyocytes with organized sarcomeres (Figure 4I), except in baseline, serum-containing conditions. These data suggest that MLC2v phosphorylation by cardiac-MLCK plays a critical role in initiating sarcomere reassembly.

Cardiac-MLCK is essential for normal cardiac development and function in zebrafish embryos. In order to further evaluate the physiologic roles of cardiac-MLCK, genetically engineered animals must be examined. In mice, however, targeted deletion of the cardiac ventricular myosin light chain, a specific substrate of cardiac-MLCK, was embryonic lethal at embryonic day 12.5 (6). Because cardiac-MLCK is an upstream modulator of MLC2v, deletion of the gene encoding cardiac-MLCK could also be embryonic lethal. Therefore, we performed in vivo knockdown experiments in *Danio rerio*, in which the phenotype generated by disrupting the functions of a targeted gene can be analyzed even if loss of the gene's functions is fatal. First, we generated a zebrafish cDNA library from which we cloned the zebrafish ortholog of *MYLK3* (*zmylk3*; encoding z-cardiac-MLCK). The amino acid sequence of cardiac-MLCK is highly similar to those of other vertebrate orthologs, especially within the C-terminal serine/threonine kinase domain (Figure 5A). Furthermore, like *MYLK3*, *zmylk3* is located between the genes VPS35 and NP001001436.1 (Assembly Zv5sc; Wellcome Trust Sanger Institute), indicating that this was the region of synteny between human and zebrafish. We also performed whole-mount in situ hybridizations using *zmylk3*-specific probes; the results indicated that *zmylk3* was expressed only in the heart at 24 and 48 hours postfertilization (hpf; Figure 5, B–I).

We injected zebrafish embryos with a specific MO directed against the AUG translational start site of the z-cardiac-MLCK mRNA (z-cMKaugMO). At 33 hpf, compared to control mock-injected zebrafish embryos, the heart region was slightly swollen in the z-cMKaugMO morphants. At 48 hpf, ventral swelling was observed in 45.6% ± 6.8% of the z-cMKaugMO morphants (Figure 6A). The ventral swelling became more apparent at 72 hpf (Figure 6B). In contrast, zebrafish embryos injected with an MO containing 5-base mismatches compared with z-cMKaugMO were indistinguishable from control zebrafish embryos (Figure 6C). We further examined the effects of 3 additional MOs, which were targeted to delete specific exons of z-cardiac-MLCK and z-MLC2v. Of these MOs, 2 were directed against the splice donor and acceptor

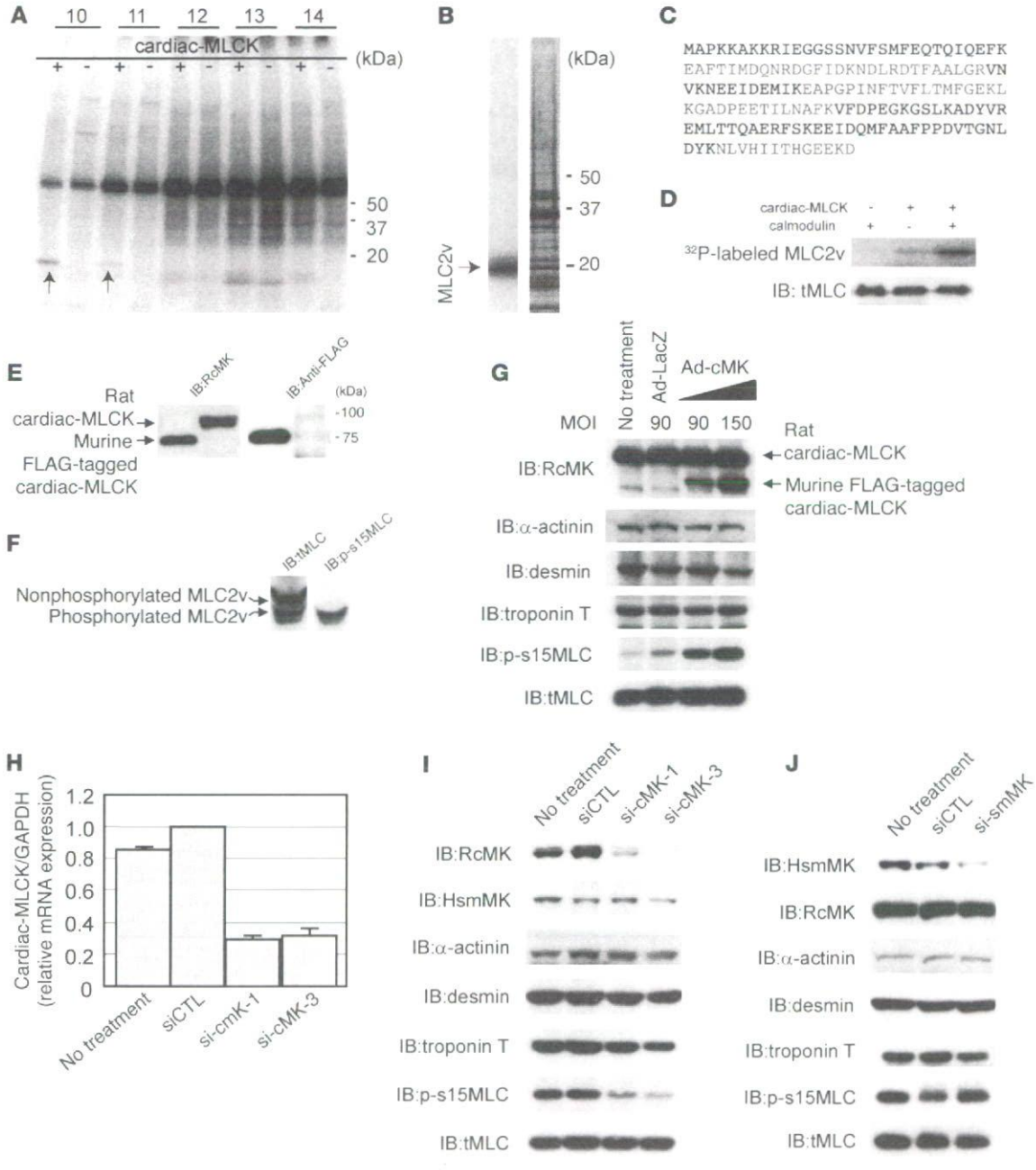

Figure 2

Identification of MLC2v as a specific substrate of cardiac-MLCK. (**A**) A putative 20-kDa substrate that was labeled with P^{32} in the presence of cardiac-MLCK was identified in fractionated murine myocardium extracts (arrows). Fraction numbers are shown at top. (**B**) P^{32}-labeled MLC2v was purified and visualized by autoradiography (left lane) and silver staining (right lane). (**C**) Peptides from the purified protein, which matched the sequences of murine MLC2v, are shown in red. (**D**) Purified MLC2v from murine myocardia was phosphorylated by cardiac-MLCK in a Ca^{2+}-calmodulin–dependent manner. (**E**) RcMK detected rat cardiac-MLCK from cultured cardiomyocyte cell extracts and FLAG-tagged murine cardiac-MLCK. (**F**) Nonphosphorylated MLC2v and phosphorylated MLC2v were separated using urea-glycerol gel electrophoresis. tMLC and p-s15MLC were confirmed to specifically detect each target protein. (**G**) Overexpression of murine cardiac-MLCK in cultured cardiomyocytes following infection with an adenovirus vector encoding murine cardiac-MLCK at MOIs of 90 and 150 upregulated the phosphorylation of MLC2v in a dose-dependent manner. Endogenous rat cardiac-MLCK is shown at top; overexpressed murine cardiac-MLCK is shown below. (**H** and **I**) Both si-cMK-1 and si-cMK-3 effectively suppressed the mRNA (**H**) and protein levels (**I**) of cardiac-MLCK, resulting in reduced phosphorylation of MLC2v. smMLCK, α-actinin, desmin, and troponin T were not affected by suppression of cardiac-MLCK expression. siCTL, control siRNA. (**J**) The protein levels of smMLCK were effectively decreased by si-smMK; no remarkable changes were observed in protein levels of phosphorylated MLC2v or other sarcomere-related proteins.

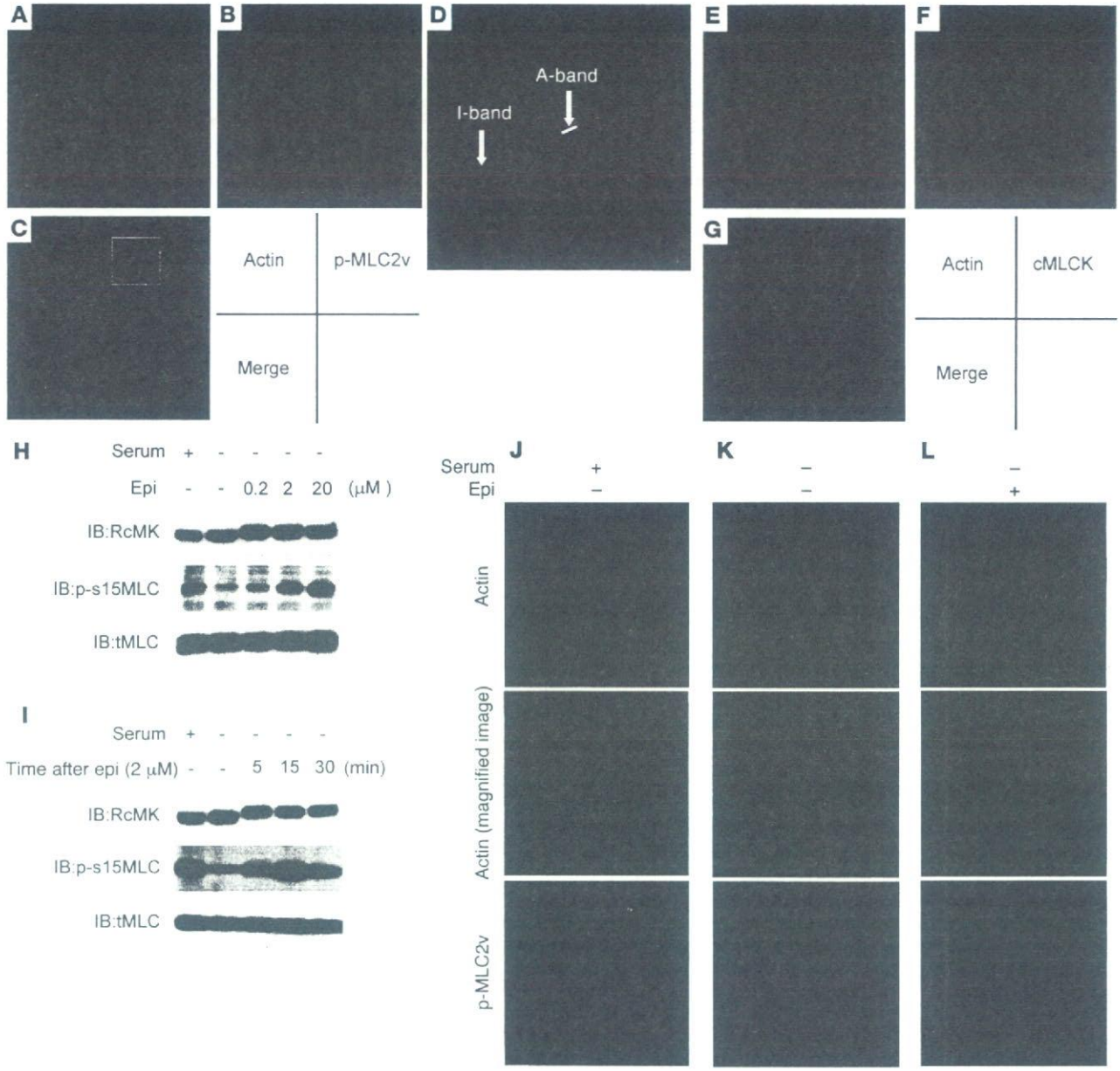

Figure 3

Epinephrine treatment induced sarcomere assembly through MLC2v phosphorylation. Original magnification, ×1,000 (**A–C** and **E–G**). (**A–D**) Polymerized actin stained with rhodamine-phalloidin (**A**) as well as phosphorylated MLC2v labeled with p-s15MLC (**B**) exhibited regular patterns of striation. (**C**) Merged image of **A** and **B**. (**D**) Higher magnification of boxed area in **C** revealed that rhodamine-phalloidin predominantly stained the I-band, whereas phosphorylated MLC2v (p-MLC2v) was localized in the A-band. Original magnification, ×4,000 (**D**). (**E–G**) Cardiac-MLCK (cMLCK) labeled with RcMK showed a diffuse cytosolic labeling pattern. (**H**) Cultured cardiomyocytes were stimulated with 0.2–20 μM epinephrine (Epi), which upregulated MLC2v phosphorylation in a dose-dependent manner. (**I**) Cultured cardiomyocytes were stimulated with 2 μM epinephrine for the indicated time periods. Epinephrine-induced phosphorylation of MLC2v in cultured cardiomyocytes was observed as early as 5 minutes after stimulation; maximal phosphorylation was obtained after approximately 30 minutes. (**J–L**) Cardiomyocytes cultured with serum contained organized patterns of striation and a moderate level of MLC2v phosphorylation. Middle panels show higher magnification of boxed regions in top panels. Cardiomyocytes cultured in serum-free conditions were incubated in the absence (**K**) or presence (**L**) of 2 μM epinephrine. (**K**) Cardiomyocytes cultured under serum-free conditions contained disorganized, punctuated actin staining with a reduced level of MLC2v phosphorylation. (**L**) Stimulation with epinephrine provoked rapid sarcomere reassembly and augmented MLC2v phosphorylation. Original magnification, ×1,000 (**J–L**, upper and lower panels); ×3,000 (**J–L**, middle panels).

sites of exons 4 and 6 of z-cardiac-MLCK, respectively. Deletion of exon 4 caused a frameshift and resulted in premature termination of the transcript. Exon 6 includes the catalytic center of z-cardiac-MLCK, and its deletion was expected to diminish the protein's kinase activity. The third MO was designed to delete exon 2 of z-MLC2v, which includes the phosphorylatable serine. These 3

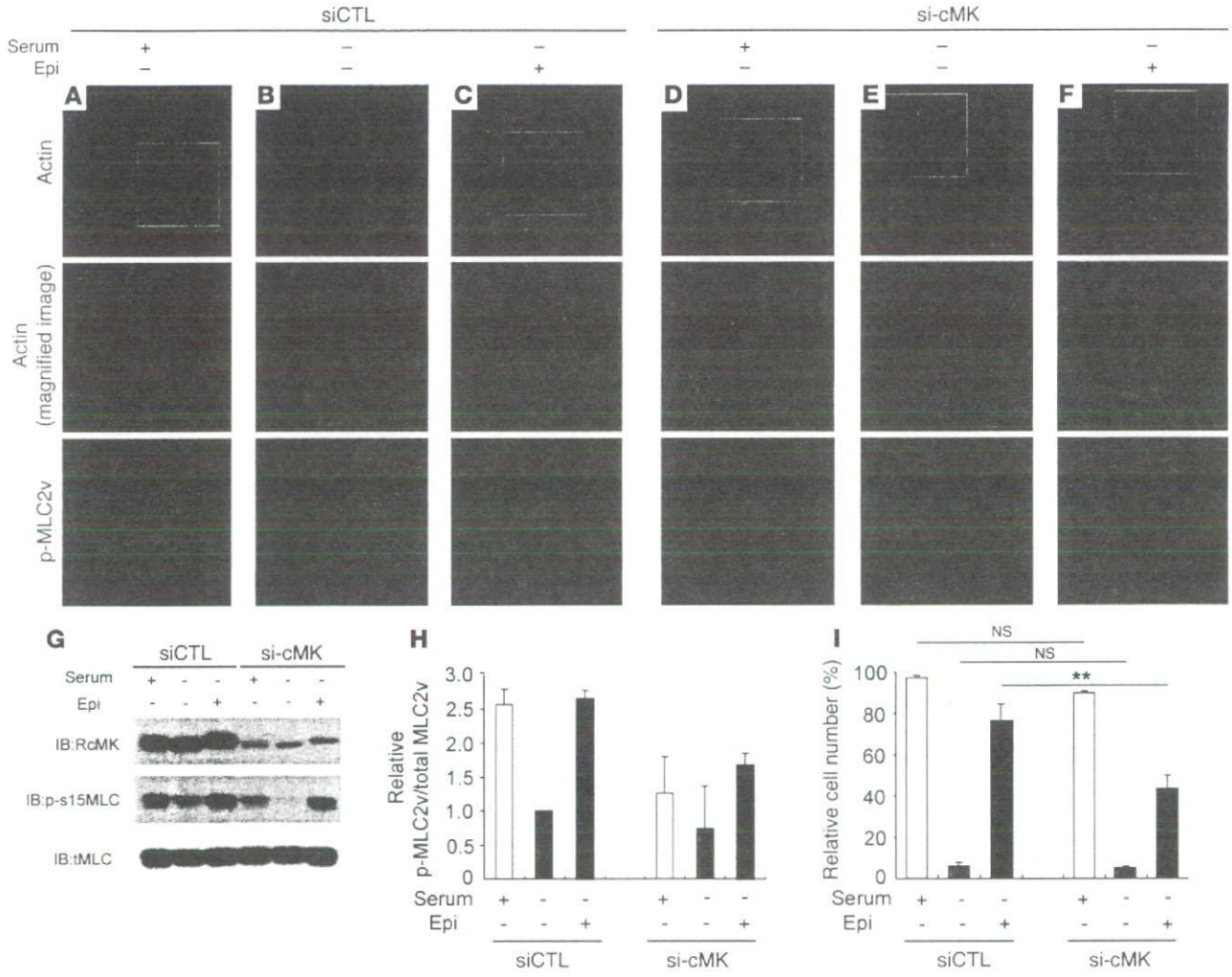

Figure 4

Cardiac-MLCK regulates the initiation of sarcomere assembly in cultured cardiomyocytes through MLC2v phosphorylation. Original magnification, ×1,000 (upper and lower panels); ×2,000 (middle panels). (**A–F**) Cardiomyocytes were transfected with control siRNA (**A–C**) or si-cMK (**D–F**). Middle panels show higher magnification of boxed regions in top panels. In serum-containing conditions, si-cMK–transfected cardiomyocytes showed reduced levels of MLC2v phosphorylation (**D**) compared with control siRNA–transfected cardiomyocytes (**A**), although both exhibited regularly organized sarcomere structures. Actin staining in cardiomyocytes cultured in serum-free conditions revealed a punctuated pattern in the sarcomeres (**B** and **E**); moreover, the degree of MLC2v phosphorylation was reduced in the si-cMK–transfected cardiomyocytes compared with the control siRNA–transfected cardiomyocytes. Stimulation with 2 μM epinephrine provoked upregulation of MLC2v phosphorylation and sarcomere reassembly in control siRNA–transfected cardiomyocytes (**C**), but not in si-cMK–transfected cardiomyocytes (**F**). (**G**) We confirmed the levels of MLC2v phosphorylation shown in **A–F** using immunoblot analysis. (**H**) Quantitation of the levels of phosphorylated MLC2v shown in **G**. Values are mean ± SEM. (**I**) Percentage of the cells with organized sarcomeres. There was no significant difference between the populations of cardiomyocytes transfected with control siRNA and si-cMK under either serum-containing or serum-free conditions. The percentage of the cells with organized sarcomeres was significantly higher for the control siRNA–transfected cardiomyocytes than for the si-cMK–transfected cardiomyocytes. Values are mean ± SEM. p-MLC2v, phosphorylated MLC2v. $^{**}P < 0.001$.

MOs effectively deleted the targeted exons, inducing comparable ventral swelling phenotypes (Figure 6, D–F). The finding that 4 different MOs produced similar results suggests that the cardiac phenotypes resulted from a loss of the kinase activity of z-cardiac-MLCK. To evaluate the cardiac phenotype of the z-cMKaugMO morphants in detail, we examined the SAG4A zebrafish strain, which specifically expresses GFP in the cardiac ventricle (14). After injecting z-cMKaugMO into SAG4A embryos, cardiac motion at 72 hpf was imaged with a high-sensitivity digital camera attached to a fluorescence stereomicroscope (Figure 6G and Supplemental Movies 1 and 2; supplemental material available online with this article; doi:10.1172/JCI30804DS1). Recordings were converted to motion mode (M-mode) images using our original software (Figure 6H). From these images, we determined the end-diastolic dimension (Dd), end-systolic dimension (Ds), and fractional shortening (FS) of the cardiac ventricle. These data are summarized in Table 2, and the results indicate that the cardiac dimensions of the z-cMKaugMO morphants were significantly larger than those of control zebrafish embryos (Dd, 79.6 ± 3.7 versus 117.0 ± 10.4 μm; Ds, 50.3 ± 6.5 versus 76.0 ± 7.0 μm; $P < 0.0001$ for both com-

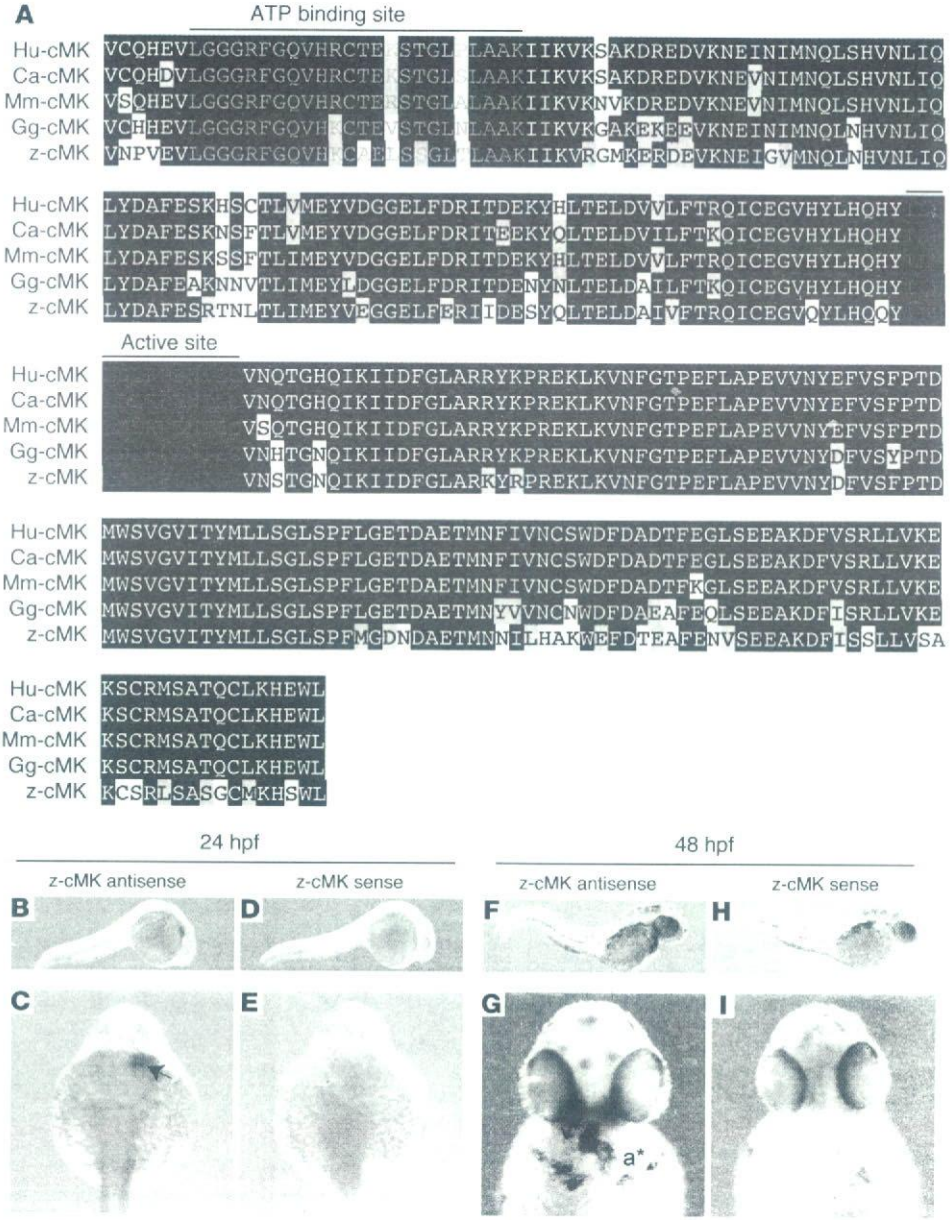

Figure 5
Cardiac-MLCK is highly conserved in several vertebrates, including zebrafish. (**A**) Cardiac-MLCK is evolutionarily conserved in vertebrates, including humans (Hu), dogs (Ca), mice (Mm), chickens (Gg), and zebrafish (z), with the highest degree of homology in the C-terminal portion of the serine/threonine kinase domain. Black backgrounds indicate identical amino acids. Amino acids in the ATP-binding region are shown in blue; those in the kinase active site are shown in red. (**B–I**) Whole-mount in situ hybridizations depict the expression of z–cardiac-MLCK (z-cMK) in zebrafish embryos hybridized with z–cardiac-MLCK–specific antisense probe (**B**, **C**, **F**, and **G**) or z–cardiac-MLCK sense probe (**D**, **E**, **H**, and **I**). At 24 hpf, z–cardiac-MLCK was expressed in heart precursor cells (arrow). At 48 hpf, z–cardiac-MLCK was selectively expressed in the heart (asterisks denote atrium [a] and ventricle [v]).

parisons). We did not, however, observe a significant difference in cardiac contractility as assessed by the FS (36.9% ± 7.1% versus 34.9% ± 4.1%; NS), likely because of a compensatory upregulation of inotropy. In support of this hypothesis, we observed that the heart rate was significantly higher in the z-cMKaugMO morphants (184 ± 14.5 versus 216 ± 24.7 bpm; $P = 0.0017$). At 5–6 days after fertilization, the z-cMKaugMO morphants developed systemic edema and died of circulatory disturbances. Histopathologic analysis demonstrated that the ventral swelling in the z-cMKaugMO morphants reflected pericardial edema. Although the cardiac atria were almost normal, the ventricular walls of the morphants were thinner than those of control zebrafish embryos (Figure 7, A–D). Transmission electron microscopy revealed that only a few poorly differentiated sarcomere structures were present in the ventricles of the z-cMKaugMO morphants (Figure 7, G–J); no other apparent abnormalities were detected in the atrial sarcomeres (Figure 7, E and F). These data suggest that cardiac-MLCK is required for sarcomere formation in the developing heart.

Cardiac-MLCK is upregulated during myofibrillogenesis and in mammalian models of heart failure. Sarcomere organization in cardiomyocytes in vivo is supposed to occur during myofibrillogenesis. In the rat heart, the mRNA and protein levels of cardiac-MLCK were upregulated from 1 week after birth through adulthood (Figure 8, A and B). The expression of cardiac-MLCK mRNA was also analyzed in mammalian models of heart failure. Myocardial infarctions (MIs) were produced in Wistar rats by permanently ligating the left anterior descending artery. At 4 weeks after the onset of MI, heart failure developed. The hemodynamic and echocardiographic parameters of the MI and sham-operated rats are summarized in Table 3. In MI rats, the LV end-diastolic pressure and LVDd were significantly higher than in sham-operated rats (LV end-diastolic pressure, 20.5 ± 8.2 versus 3.2 ± 1.0 mmHg; $P < 0.01$;

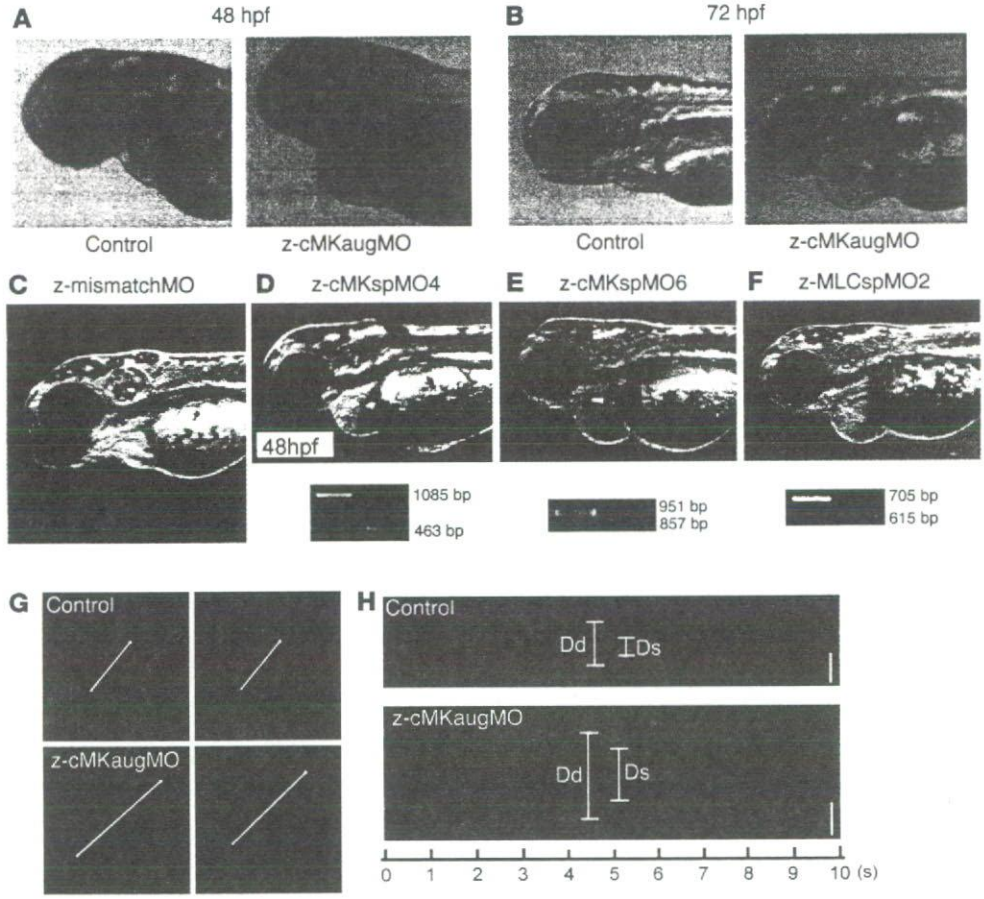

Figure 6

Suppression of z–cardiac-MLCK expression induced dilatation of the cardiac ventricle in zebrafish embryos. (**A** and **B**) Control mock-injected zebrafish embryos and zebrafish embryos injected with z-cMKaugMO produced the phenotype of ventral swelling at 48 hpf (**A**) and 72 hpf (**B**). (**C**) Zebrafish embryos injected with MOs with 5-base mismatch to z-cMKaugMO (z-mismatchMO) showed phenotypes comparable to those of controls. (**D** and **E**) Injection of specific MOs designed to interfere with the splicing of z–cardiac-MLCK exon 4 (z-cMKspMO4; **D**) or exon 6 (z-cMKspMO6; **E**) or with the splicing of z-MLC2v exon 2 (z-MLCspMO2; **F**), which coded for the phosphorylatable serine residue, also induced the phenotype of ventral swelling. RT-PCR products amplified from cDNA produced from the morphants were shorter than those obtained from control embryos due to the removal of the targeted exons. (**G**) Cardiac motion in the control embryos and z-cMKaugMO morphants. Shown are end-diastolic (left) and end-systolic (right) phases of the cardiac ventricular cycle in a control embryo and z-cMKaugMO morphant. (**H**) Representative M-mode images of both control embryo and z-cMKaugMO morphant hearts. Scale bars: 50 μm. Original magnification, ×20 (**A**–**F**); ×100 (**G**).

LVDd, 9.8 ± 0.3 versus 6.8 ± 0.5 mm; $P < 0.01$), whereas the maximum LV peak rate of change in pressure during isovolumic contraction (Max dP/dt) and FS were significantly lower than in sham-operated rats (Max dP/dt, 5,845 ± 1,156 versus 9,440 ± 644 mmHg/s; $P < 0.01$; FS, 12.0 ± 3.1 versus 44.0 ± 7.8%; $P < 0.01$). In MI rats, *MYLK3* expression was significantly upregulated compared with that in the sham-operated rats (relative cardiac-MLCK mRNA expression, 1.46 ± 0.42 versus 1.00 ± 0.15; $P < 0.05$; Figure 8C). Furthermore, the relative mRNA expression level of cardiac-MLCK was significantly correlated with that of ANP ($r = 0.778$, $P < 0.005$; Figure 8D). Upregulation of cardiac-MLCK expression in the infantile heart suggests cardiac-MLCK participates in myofibrillogenesis. Additionally, upregulation of cardiac-MLCK mRNA levels in mammalian models of heart failure confirmed the results obtained with the microarray analysis of human failing myocardia.

Discussion

In this study, we performed microarray analysis of human failing myocardia to identify new genes involved in the pathophysiology of CHF. By comparing mRNA expression analysis with the clinical parameters of the patients, we identified what we believe to be a novel candidate gene, *MYLK3* (encoding cardiac-MLCK), that had not been isolated in previous microarray studies of heart failure (15). Upregulation of *MYLK3* transcription in failing myocardia was confirmed in mammalian models of heart failure, such as MI rats. In this experiment, mRNA expression of cardiac-MLCK was significantly upregulated in MI rats with heart failure, and the relative expression profile was well correlated with that of ANP, a representative marker of CHF.

MLCK family members in muscle are sarcomeric protein kinases that phosphorylate a serine residue near the amino terminus of the myosin regulatory light chain. In cardiac muscle, phosphorylation of MLC2v led to sarcomere organization, an event that represents cardiac hypertrophy in cultured neonatal rat cardiomyocytes (13). skMLCK is thought to be the predominant kinase that acts on MLC2v, and a gradient of MLC2v phosphorylation in the cardiac wall from endocardium to epicardium is responsible for the generation of cardiac torsion (9). A recent study using skMLCK-deficient mice, however, revealed that removing skMLCK did not result in a cardiac phenotype (10). Furthermore, in the current study and previous studies, skMLCK expression was not detected in the heart by either Western blotting or RT-PCR (16), suggesting the existence of an as-yet unknown kinase that phosphorylates MLC2v in cardiac muscle.

We identified cardiac-MLCK, which serves as a specific kinase for MLC2v in cardiac muscle. In cultured cardiomyocytes, cardiac-MLCK regulates sarcomere assembly through the phosphorylation of MLC2v. When isolated cardiomyocytes were cultured under serum-free conditions, established sarcomere structures were disrupted. Overexpression of recombinant cardiac-MLCK and exogenous stimulation by epinephrine promoted sarcomere